

ANALYSIS OF FLOW PATTERNS DURING ROLLING USING SOFTWARE PACKAGES

A DISSERTATION

*Submitted in partial fulfilment of the
requirements for the award of the degree*

of

MASTER OF ENGINEERING

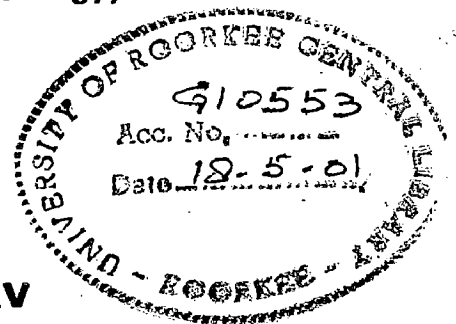
in

METALLURGICAL ENGINEERING

(With Specialization in Physical Metallurgy)

By

SATYA PRAKASH YADAV



**DEPARTMENT OF METALLURGICAL AND MATERIALS ENGINEERING
UNIVERSITY OF ROORKEE
ROORKEE-247 667 (INDIA)**

FEBRUARY, 2001

CANDIDATE'S DECLARATION

I hereby certify that the work presented in the dissertation entitled, "ANALYSIS OF FLOW PATTERNS DURING ROLLING USING SOFTWARE PACKAGES", in partial fulfilment of the requirements for the award of the degree of MASTER OF ENGINEERING in METALLURGICAL ENGINEERING with specialization in the PHYSICAL METALLURGY, submitted in the Department of Metallurgical and Materials Engineering, University of Roorkee, Roorkee is an authentic record of my own work carried out from August 2000 to February 2001, under the supervision of **Dr. R.P. Ram**, Associate Professor, Department of Metallurgical and Materials Engineering, University of Roorkee, Roorkee.

The matter embodied in this dissertation has not been submitted by me for award of any other degree or diploma.

Satya Prakash Yadav

Place : Roorkee

(SATYA PRAKASH YADAV)

Dated : February 28 , 2001

CERTIFICATE

This is to certify that the above statement made by candidate is correct to the best of my knowledge.

Dr. R.P. Ram

Dated : February 28 , 2001

(Dr. R.P. Ram)
Associate Professor,
Deptt. of Met. & Mat. Engg.
University of Roorkee,
Roorkee – 247667 (India)

ACKNOWLEDGEMENT

I am greatly indebted to my guide Dr. R. P. Ram, associate professor, University Department of Metallurgical And Materials Engineering of Roorkee, Roorkee for his kind support and guidance during my work. His co-operation and in-depth knowledge has made my work possible.

I am thankful to Mr. Narendra Kumar, for giving me the complete freedom for doing work in the lab at any time.

Last but not the least, I am also profoundly grateful to all the teachers at this department and to my friends who have helped me in this thesis work and without whose untiring help and support, this work would have remained a distant dream.

Satya Prakash Yadav

DATE: 28th Feb 2001

SATYA PRAKASH YADAV

Errata -1

Page No.	Line No.	Written Word	Read as
7	5	marketing	marking
7	10	agramatic	diagrammatic
15	11	visioplsticity	visioplasticity
17	3	Sakeskin	Snakeskin
31	11	takes	take
31	15	exist	exists
33	5	exit	exists
35	1	GEOREG	GEORGE
35	5	TMOMPSEN	THOMPSEN

Errata-2

The Part Added In Results And Discussion

It is clear from the figures 8-14 that as the reduction ratio increases, the contact angle also increases. It can be also deduced from the tables 2-4. Therefore higher reduction ratio in the rolling makes larger contact angle. It can be achieved either by reducing roll diameter or by increasing friction between the roll and strip. This is the reason why grooved rolls are used in the rolling operations.

From the tables 1-4, it can be said that moving from the entrance to the exit in the second zone, the velocity increases gradually and direction of the velocity changes gradually.

From the figures 8-22 it is deduced that when contact angle is small, the material near the surface of the roll flows parallel to roll surface and defectless rolled product is obtained. But when the contact angle is larger than a certain critical value α_1 ($\alpha_1 > \alpha_{opt}$), a dead metal zone forms, as shown in figure 37. The material adjacent to the roll adheres to it and is immobilized, forming a die like surface. If the contact angle increases further beyond a certain critical value α_2 ($\alpha_2 > \alpha_1$), a chip rolled product will be formed as shown in figure 38. The roll acts as a cutting tool in orthogonal cutting, shaving off the surface of the strip. The

chips flow over and away from the surface of the roll, leading to wastage of material.

Larger reduction requires higher pressure on the rolls. Larger pressures on the rolls cause more and more flattening and bending of the rolls. When excessive pressure is limiting the maximum reduction, it is said that limiting reduction or limiting thickness is reached. The front and back tensions are applied to reduce the pressure on the roll.

ABSTRACT

The work was necessitated keeping in view the shop floor practice of the metal forming problems. A suitable software is developed for the analysis of flow through rolling. C++ programming language and C++ graphics are used as a tool to solve the problem.

Results are presented in tabular and graphics form. Possible variables and their effects on the forming operations are discussed in light of available theoretical knowledge. A number of defects of common occurrence in forming practice have been tried to be related with one or the other possible variables. It is observed that with the help of suitable formulation of the problems in the metal forming operations and subsequent utilization of these for modeling and simulations is adaptable not only in practice but it can also help in obtaining analytical solutions for a number of situations as well.

CONTENTS

CANDIDATE'S DECLARATION	(i)
ACKNOWLEDGEMENT	(ii)
ABSTRACT	(iii)
CONTENTS	(iv)
CHAPTER – 1 : INTRODUCTION	1
1.1 Upper and Lower Bound Technique	3
1.2 The Equilibrium Method	4
1.3 The Slip Line Field Theory and Analysis	5
1.4 Finite Element Method	6
1.5 Visioplasticity	7
CHAPTER – 2 : LITERATURE SURVEY	10
2.1 Approaches	10
2.1.1 Approaches Based on Finite Element Method	10
2.1.2 Approaches Based on Upper Bound Technique	12
2.1.3 Approaches Based on Equilibrium Method	14
2.1.4 Approaches Based on Visioplasticity	15
2.1.5 Approaches Based on Slip Line Field Theory	16
2.2 Defects, Irregularities their Causes and Remedies	17
2.2.1 Snakeskin, Fishskin or Fir Tree Defect	17
2.2.2 Central Bursting or Chevroning	17
2.2.3 Cavity and Piping Defect	17
2.2.4 Brittle Fracture	18
2.2.5 Yield at the Entrance or Exit Beyond the Zone of the Die	18

CHAPTER – 3 : FORMULATION OF THE PROBLEM	19-20
CHAPTER – 4 : SIMULATION STUDIES	21
4.1 Assumptions	22
4.2 Limiting Thickness and Limiting Reduction	24
4.3 Process Variables	25
4.4 Intermediate Distortion Analysis	26
4.5 Velocity Field Analysis	27
4.6 Computation of Various Parameters Involved	28
4.7 Optimal Roll Radius	29
4.8 Dead Zone Formation	29
4.9 Flow Chart of the Program	30
CHAPTER – 5 : RESULTS AND DISCUSSION	31
CHAPTER – 6 : CONCLUSION	33
CHAPTER – 7 : SUGGESTION FOR THE FUTURE WORK	34
REFERENCES	35-36
FIGURES	44-83
CODE OF C++ PROGRAM	37-43

In recent years, the metal forming industry has been striving for quality improvement and cost reduction to meet the increasingly stringent specification requirements and strong competition in the world market. The industry has recognized that effective quality and cost reduction can only be achieved by an improved understanding of the interwoven relations among processing conditions, behavior of metal flow, and tool/metal interactions. In the past it has been demonstrated in the area of metal forming that computer modeling using numerical methods can provide detailed information of flow behavior of metals.

Metal forming operations are the methods of fabricating the materials into desired shape and size with required properties and they handle large proportions of the required products as compared to other forming methods like casting and powder metallurgical operations. The Process of plastically deforming metal by passing it between rolls is known as rolling. This is the most widely used metalworking process because it lends itself to high production and close control of the final product. In deforming metal between rolls, the work is subjected to high compressive stresses from the squeezing action of the rolls and to surface shear stresses as a result of the friction

between the rolls and the metal. The frictional forces are also responsible for drawing the metal into the rolls. The development of theoretical methods to be applied to metal forming has provided useful information about the mechanics of the processes. In the last few years rolling has been extensively analyzed mainly through the upper bound technique and the finite element method [1,2]. With the F.E.M., the velocity, strain rate, strain and stress field can be obtained in the plastically deformed material. Although this method is very powerful it requires large amount of computer capabilities. The upper bound technique is based on a kinematically admissible velocity field, which has to be assumed, the strain rates and strain fields can be derived and the upper bound load is calculated.

Manufacturing in metal forming is done in two states:

1. Axisymmetric state.
2. State of plane strain.

The processes like forming of disks, flow through conical converging dies, extrusion, tube sinking and expanding fall in the category of axisymmetric state while forging of strip, flow through inclined planes and strip rolling come into the category of state of plane strain.

The process like wire drawing, extrusion, tube sinking etc. involve the analysis of distribution of stresses in the materials being formed with two aims:

1. To prevent the failure of material during the forming operations and at the same time to guarantee a defect less product.
2. To obtain a product with desired mechanical and other properties.

For the analysis of the above processes at any level there are generally five approaches, which are used as follows:

- Upper and lower- bound technique.
- The equilibrium method.
- The slip line field theory and analysis.
- Finite element method
- The Visioplasticity

Irrespective of the method of analysis adopted, the basic characteristics of the plastic state of material will have to be assumed, namely

- The condition of constancy of volume.
- The yield criterion and the functional yield or flow or representative stress relations.

1.1 UPPER AND LOWER-BOUND TECHNIQUE:-

This approach is fully used, will produce two expressions for the load required, the so called lower bound and the upper bound. The former underestimates the load required whereas the latter gives the realistic over estimate of the problem.

The upper bound approach is not concerned with conditions of stress equilibrium but only with the conditions that should be fulfilled by the strain increments in the material undergoing full plastic deformation. This in turn involves the consideration of a kinematically admissible velocity field i.e. the consideration of a distribution of generalized particle velocities, which is kinematically compatible within itself and also with the velocities, applied externally to the boundaries.

To obtain a solution the working region of a pass is divided into a number of zones inside which the particle velocity is continuous. Discontinuities may be present in adjacent zones but this may occur in tangential components of the velocity along the actual zone interfaces and tool specimen boundaries. Discontinuities imply the presence of shear and the existence of velocity distribution in each zone indicates the presence of plastic strain and consequently dissipation of energy.

Since energy is governing factor in changing the shape of material body, computation of this quantity will be instrumental in defining the magnitude of external load required.

1.2 THE EQUILIBRIUM METHOD: -

This method is based on the stress field developed in the processed material. It consists of isolating representative volume element in the body of the material undergoing plastic deformation and in observing the behavior of this element as it moves along the working zone of the pass.

Basically this method requires that the conditions of force equilibrium be established in three directions i.e. $\sum f_x = \sum f_y = \sum f_z = 0$ or in, say cylindrical co-ordinate, $\sum f_r = \sum f_\theta = \sum f_z = 0$

The equation of equilibrium of forces in one direction is given by

$$\frac{\sigma_r - \sigma_\theta}{r} + \frac{\partial \sigma_r}{\partial r} - \frac{2\tau}{t} = 0 \quad (1.1)$$

The relationship between the stresses produced is established by means of a suitable criterion of yielding, ultimately related to tensile/compressive or shear yield stress of material.

The method is only approximate. It is, for instance, particularly suitable for wire and tube drawing, hot and cold rolling of strip and sheet and also gives an acceptable degree of approximation in rotary piercing and elongation of seamless tubing.

1.3 THE SLIP LINE FIELD THEORY AND ANALYSIS:-

It is based on the physical observation that plastic flow occurs predominately as a result of microscopic slip along crystallographic planes. This method forms a useful tool in the general field of metal forming mainly by virtue of giving some insight into the pattern of flow of material.

To obtain a solution, families of curvilinear or straight lines are constructed that intersect orthogonally and correspond to directions of maximum and minimum constant shear lines. Static equilibrium, the yield condition and the pattern of flow in the plastic zone will have to be satisfied by the assumed network of these lines. The mutually perpendicular lines in X-Y planes are designated as alpha and beta as shown in figure 2.

1.4 FINITE ELEMENT METHOD:-

The finite element ^{method} is a numerical in which the governing equations are represented in the matrix form and as such are well suited to the solution by digital computer. The solution region is represented (idealized) as an assemblage of small sub-regions called finite elements. When applied to the analysis of a continuum, the idealized region becomes an assemblage of a discrete number of elements each with a predetermined number of degrees of freedoms and can take various forms, e.g. spring, rod, membrane, etc.

Elements are considered to be connected at discrete joints (corners, intermediate points) known as nodes. Implicit with each element type is the nodal force-displacement relationship, namely the element stiffness property. Analysis requires the assembly and solution of a set of simultaneous equations, to provide the displacements for every node in the model. Once the displacement field is determined, the strains and hence stresses can be determined, using the strain- displacement and stress- strain relations.

1.5 VISIOPLASTICITY: -

It was developed by Thompsen and makes use of experimental observations of flow patterns and provides means of deriving complete solutions after, however, the experimental data have been obtained. It gives an exact solution. The technique is based on the examination of velocity field developed incrementally within the deforming body. In a general axisymmetric case a marketing grid pattern is imprinted on the meridian plane of a cylindrical work piece undergoing a metal forming operation, and the latter is conducted by imposing a unit strain at a time. A record of the change in the grid after an increment of strain has been imparted, will give a sufficient clear picture of the instantaneous pattern of flow.

To determine stress and strain –rate fields let us consider the general agrammatic Particle velocity field of figure 3. If V is a known or measurable instantaneous velocity of a particle whose position is defined by coordinates, r, θ and z , and u and v are the components of V in directions z and r respectively, then plots of u and v against, in turn, r and z can be constructed. Strain rates at point A, and at any other point in the deforming material, can be determined from the slopes of these curves. The rates will be given by

$$\dot{\epsilon}_z = \frac{\partial u}{\partial z} \quad \dot{\epsilon}_r = \frac{\partial v}{\partial r} \quad \text{and} \quad \dot{\gamma}_{zr} = \frac{\partial u}{\partial r} + \frac{\partial v}{\partial z} \quad (1.2)$$

If we assume the material to be homogeneous and isotropic ,the directions of principal stresses will be

$$\tan 2\alpha_z = \frac{\dot{\gamma}_{zr}}{\dot{\epsilon}_z - \dot{\epsilon}_r} \quad (1.3)$$

Where α_z is the angle between the z-axis and the direction of a principal stress.

The strain-rate component can be found from the condition of incompressibility

$$\dot{\epsilon}_z + \dot{\epsilon}_r + \dot{\epsilon}_\theta = 0 \quad (1.4)$$

and the effective strain rate will be given by

$$\dot{\epsilon} = \frac{\sqrt{2}}{3} \left[(\dot{\epsilon}_z - \dot{\epsilon}_r)^2 + (\dot{\epsilon}_r - \dot{\epsilon}_\theta)^2 + (\dot{\epsilon}_\theta - \dot{\epsilon}_z)^2 + \frac{3}{2} \dot{\gamma}_{zr}^2 \right]^{1/2} \quad (1.5)$$

and the effective stress is given by

$$\bar{\sigma} = \frac{1}{\sqrt{2}} \left[(\sigma_z - \sigma_r)^2 + (\sigma_r - \sigma_\theta)^2 + (\sigma_\theta - \sigma_z)^2 + 3\tau_{zr}^2 \right]^{1/2} \quad (1.6)$$

$$\sigma_z = \frac{2}{3} \int_1^r \left[\frac{\partial}{\partial r} \left(\frac{\dot{\epsilon}_z - \dot{\epsilon}_r}{\dot{\epsilon} / \bar{\sigma}} \right) - \left(\frac{\dot{\epsilon}_r - \dot{\epsilon}_\theta}{r \dot{\epsilon} / \bar{\sigma}} \right) - \frac{1}{2} \frac{\partial}{\partial z} \left(\frac{\dot{\gamma}_{zr}}{\dot{\epsilon} / \bar{\sigma}} \right) \right] dr - \frac{1}{3} \int_{z_0}^z \left[\frac{\partial}{\partial r} \left(\frac{\dot{\gamma}_{rz}}{\dot{\epsilon} / \bar{\sigma}} \right) + \frac{\dot{\gamma}_{rz}}{r \dot{\epsilon} / \bar{\sigma}} \right] dz + \sigma_{z_0} \quad (1.7)$$

σ_{z_0} is known stress related to the conditions obtained at the entry to the working zone of the considered pass.

It is clear that because of its complexity equation (1.7) will have to be integrated either numerically or graphically. In fact the use of a computer will ensure a high degree of accuracy. Equation (1.7) is of course easily reducible to conditions of plane strain if these become characteristics of the operation considered.

Although, as we have said, the viscoplasticity method gives very satisfactory results, it has been applied mainly to various extrusion problems. This appears to be due partly to the labour involved in the measurements necessary to establish the u, v versus r, z relations, and partly to the actual integration of the final expression.

As already stated, irrespective of the method of analysis adopted the basic characteristics of the plastic state of the materials will have to be assumed, as could be clear by the brief survey of the approaches adopted by various authors, namely:

- Condition of constancy of volume
- Yield criteria and the functional yield or representative stress relation

2.1.1 APPROACHES BASED ON FINITE ELEMENT METHOD:-

The finite element method is a numerical method in which the governing equations are represented in the matrix form and as such are well suited to the solution by digital computer. More recent advances in computer graphics and availability of powerful computer workstations have given even greater emphasis to the spread of finite element methods throughout engineering practice.

Two different approaches, namely the “flow approach” and the “solid approach” have emerged for the simulation of metal forming processes using the finite element method. In the flow approach, the material is assumed to behave like a non-Newtonian viscous or visco-plastic fluid and the finite element solution is obtained by

using an Eulerian reference frame (stationary mesh) as in the work of Zienkiewicz and Godbole (1974) and Dowson and Thompson (1978). It has been observed that, in spite of the capability of the Eulerian finite element mesh to represent internal deformation effectively, it is not very suitable for domains with substantially moving boundaries or interfaces. The "solid" approach on the other hand, treats the material as an elastic-plastic /viscoelastic solid and has gained relative popularity in the area of forming simulation. In this approach, a Lagrangian description (total or updated) has been traditionally used for analysis of large deformation problems by a number of researchers e.g. Yamada et.al. (1978). In this description, the finite element mesh remains embedded and moves with the material constituting the continuum.

A finite element method for limit analysis of plain strain extrusions through square dies by K.K.Liu and W.H.Yang [3], have developed general limit analysis algorithm and has been applied to plane strain extrusion through dies. The method is based on a duality theorem and an iterative minimization procedure. In each step of iteration, a constrained quadratic optimization problem is solved by the penalty function method with the reduced integration technique. Solutions are presented in terms of limit extrusion pressure and the corresponding velocity. Results obtained are compared with the available classical slip line solutions and are found to be in good agreement.

Application of the finite element method to the simulation of rolling process of flat and long products by E..Amici, G. Demofonti, M.Lubrano & C.Pietrosanti and

N.Kapaj [3] have developed the simulation of rolling of small thickness product with a 2-d schematization for different reduction ratios, followed by the rolling of large thickness products and 3-d rolling, simulating the rolling of long products.

2.1.2 APPORACHES BASED ON UPPER BOUND TECHNIQUE:

This approaches if fully used will produce two expressions for the load required the so- called lower and upper bound. The former underestimates the load required whereas the latter gives the realistic overestimates of the problem.

The upper bound approach is not concerned with conditions that should be fulfilled by the strain increments in the material undergoing plastic deformation. These in turn involve the consideration of a distribution of generalized particle velocities, which is kinematically compatible within it and also with the velocities applied externally to the boundaries.

Manabu Kiuchi and Michihiko Hoshino [3] have developed the computer- aided simulation based on upper bound theorem to analyze their dimensional flow of work pieces in various extrusion processes.

The developed method is applied to simulation of forward extrusion of tubes through bridge dies. The effect of die geometry on extrusion pressure, geometry of dead zone, plastic zone and three dimensional flow of workpieces evaluated on the results match with the experimental evidences.

B.. Avitzur [2] writes that in the operations of tube forming , in order to change the diameter of the tube , tube is drawn through a conical die(tube sinking)to decrease its diameter. An upper bound approach to the energy consumption is utilized.

The required operational stresses are computed. The maximum possible reduction in area, or maximum diametrical ratio is determined and the optimal cone angle is evaluated.

B.Avitzur [8] did his work on " Analysis of wire drawing and extrusion through conical dies of large cone angle" in which the operation of wire drawing and extrusion through conical dies was treated on the assumption that mises materials are formed. An Upper bound solution is obtained for the drawing stress in wire drawing and for the pushing stresses in extrusion. The effect of each of the process variables on these forces was studied.

The process variables are the cone half angle (α), initial radius (R_i) and final wire radius (R_f) material yield limit (σ_o) under uniaxial load, back pull ($\sigma_{.tb}$) and front pull ($\sigma_{.xf}$), coefficient of friction (μ) or shear factor (m), die land (L), exit velocity (V_f). On the assumption that the maximum front tension can not exceed the yield limit of the material under uniaxial tension, a solution is obtained for maximum possible reduction in wire drawing. An analogous assumption that the

absolute value of pushing stress also cannot exceed the yield value, gives a criteria for maximum possible reduction in extrusion.

2.1.3^A APPROACHES BASED ON EQUILIBRIUM METHOD:-

This method is based on the stress field developed in the processed material. It consists of isolating representative volume element in the body of the material undergoing plastic deformation and the behavior of this element as it moves along the working zone of the pass.

C.T.Yang [5] uses the equilibrium method to find the coefficient of friction in wire drawing in "On the mechanics of wire drawing". The effect of the parallel portion of die on the coefficient of friction obtained, the drawing stresses were calculated from the derived equations.

A.H.Shabik and E.G.Thomsen [6] have analyzed the theoretical and experimental flow field of several extrusion ratio of lead extruded in plain strain comparatively. The two methods are derived from the equations describing the mechanics of the process. The differential equation in the flow function was used to obtain the flow lines. Excellent agreement was found when both the flow lines and the velocity components matched with those obtained experimentally. The experimental and the theoretical solutions obtained are both unique and complete.

2.1.4 APPROACHES BASED ON VISIOPLASTICITY:-

This technique is based the examination of a velocity field developed incrementally within the deforming body and gives an exact solution. Von Houlte. P.Watte. P.Aernoudt, E.Sevillano, J.Gil.Lefever [8] did their work on "Taylor simulation of cyclic textures at the surface of drawn wires" and have simulated the deformation textures, which were developed during wire drawing at the surface of pearlitic carbon steel by means of Taylor theory. These surface textures do not have a full rotational symmetry such as fiber textures found in the center of drawn wires. This effect was believed to be caused by more complex material flow, which exists near the surface in comparison to the center.

A.Shaibak and S.Kobayashi [14] did their work on the " computer application to the visioplsticity method", in which procedures for using a computer for the complete solution of plane strain as well as axisymmetric deformation problem have been developed. The velocity, strain rate, total effective strain, and stress distributions were obtained for two commercially pure lead specimens extruded in a forward extrusion process using white lead in oil as a lubricant. The axisymmetric extrusion was carried out at a speed of 1/8 ipm through angle with a 2:1 extrusion ratio and the plain - strain extrusion through a tapered die having a 45-degree half-taper angle with a 1.66:1 extrusion ratio.

A.Leopold, Juergen, Guerthen and Holger [15] have proposed a solution for the recognition of points in large deformed and injured lattices using digital image

processing in combination with neural networks. The viscoplasticity finds application in analysis of large plastic deformation in metal cutting and forming processes and for quality control.

2.1.5 APPROACHES BASED ON SLIP LINE FIELD THEORY:-

The first approach to the analysis of the metal working process that did not assume homogeneous uniform deformation was slip line field theory. The slip line fields account for inhomogeneous deformation in the calculation of the overall forming loads. For many metalworking processes there are no slip line fields to allow prediction of stresses. Moreover, slip line fields are valid only for the plain- strain conditions [1].

G.W. Rowe [7] has applied slip line field theory to study steady state motion of 50% inverted extrusion in plain strain with lubricated dies. Die was assumed to be at rest with the billet end container moving towards it with unit velocity.

It is based on the physical observation that plastic flow occurs predominantly as a result of microscopic slip along crystallographic planes. This method forms a useful tool in the general field of metal forming mainly by the virtue of giving some insight into the pattern of the flow of material.

2.2 DEFECTS, IRREGULARITIES, THEIR CAUSES AND REMEDIES

2.2.1 SNAKESKIN, FISHSKIN OR FIR TREE DEFECT:-

Sakeskin or fishskin defect occurs when the core of the product flows faster than the skin. The skin might then break. Because of its appearance it is given the name. This defect appears only when unique combination of variables develops during the processing. The rules that govern the formation of this defect are not well understood. A costly trial and error method is followed for its prevention.

2.2.2 CENTRAL BURSTING OR CHEVRONING:-

When the center of the billet fractures rather than the skin, the skin flows out faster than the core and central bursting occurs. When this defect occurs, changing the reduction ratio or cone angle to stay away from the danger is advocated.

2.2.3 CAVITY AND PIPING DEFECT:-

The cavity starts as a little dimple on the back of the billet. With the squared dies, cavity starts early when the billet is still long. It increases rapidly and develops into the piping defect. By decreasing the cone angle, flow becomes more uniform, initiation of cavity is delayed, and the piping defect may be prevented.

2.2.4 BRITTLE FRACTURE:-

Brittle fracture of hard to deform materials can be prevented by the use of backpressure in the exit chamber. It is seen that even without backpressure, brittle fracture can be avoided by the proper choice of reduction. The choice of cone angle can aid plastic flow without fracture.

2.2.5 YIELD AT THE ENTRANCE OR EXIT BEYOND THE ZONE OF THE DIE:-

In wire drawing the limit on the drawing stress is given by the yield limit of the material, when the required drawing stress is higher than the yield limit of the material the wire will not flow through the die, instead the die will stop it and wire at exit will break down and tear. If the backpressure is higher than the yield value, the billet will be stopped by the die and barrel at the entrance. A further limitation is imposed on the length of billet that can be extruded without buckling. Buckling can be overcome by a suitable design of supports.

The equations used for the present work are,

$$\dot{U}_r = \frac{V_f t_f}{R_{RO}} \left(\frac{1}{t_f / R_{RO} + \alpha_n^2} \right) \quad (3.1)$$

$$\left(\frac{R_{RO}}{t_f} \right)_{opt} = \frac{1}{\left(m \left(\frac{t_o}{t_f} - 1 \right) \right)} \quad (3.2)$$

$$\text{The Contact Angle } \alpha_2 = \sqrt{\frac{t_f}{R_{RO}}} \sqrt{\frac{t_o}{t_f} - 1} \quad (3.3)$$

In the Strip Rolling the thickness t_o , the ratio ($t_f / R_{RO} \ll 1$), and the reduction are small ($t_o / t_f - 1 \ll 1$). Equation (3.3) states that the contact angle in strip rolling is small.

$$\alpha_{opt} = -\frac{t_f}{3mR_{RO}} \left[\ln \left(\frac{t_o}{t_f} \right) + \frac{1}{4} \sqrt{\frac{t_f}{R_{RO}}} \sqrt{\frac{t_o}{t_f} - 1} + \frac{\sigma_{xb} - \sigma_{sf}}{(2/\sqrt{3})\sigma_o} - m \sqrt{\frac{R_{RO}}{t_f}} \tan^{-1} \sqrt{\frac{t_o}{t_f} - 1} \right] \quad (3.4)$$

Zero strain rates exist in zone first and third, where there is no work of deformation as shown in figure 4. The strain rate for zone second is:

$$\dot{\epsilon}_R = -\dot{\epsilon}_\theta = 2 \left(\frac{t_f}{R_{RO}^2} \right) \dot{U}_r \frac{\alpha}{\left(t_f / R_{RO} + \alpha^2 \right)^2} \quad (3.5)$$

All other $\dot{\epsilon}_{ij} = 0$

Equation (3.5) gives the deformation in second zone. With the help of stress analysis of second zone during deformation, the actual values of involved parameters at different points in the second zone can be known. C++ programming language and C++ graphics can be used as tool for solving the problem. In the problem the deformation zone is divided into grid points by the various combination of r and θ , and at these points the value of strain rates are calculated by the software and these values are plotted at various grid points in the space. Mathematical relations for the problem are taken from B. Avitzur [2], which are modelled forms for the situations.

The approach for the development of the software is three fold. A program for the evaluation and depiction of material velocity U_r , radial strain rate $\dot{\epsilon}_R$, angular strain rate $\dot{\epsilon}_\theta$ has been made after the calculation of optimal roll radius $(R_{ROLL})_{opt}$. This part of the approach of the development of program was chosen to aim at the follow up of some of the process variables together with the most vital flow pattern variables of the process.

The second part of the approach for the development takes into account a non-optimal semi die cone angle. Under the second condition, the importance for the flow pattern variables of the materials e.g. $\dot{\epsilon}_R, \dot{\epsilon}_\theta, U_r$ were tried to be emphasized.

The third part of the program deals with the drawing of displacement contours as the element flows through the deformation zone. It also tabulates the various time periods taken to cross the respective deformation zones. Visioplasticity method is preferred over other methods like finite element method to solve problem. The reason is that the contours drawn in this case are two-dimensional which can be easily shown in dynamic mode. This enables the user to interpret the contours in a much easier way.

4.1 ASSUMPTIONS:-

To simplify the complexities, the following four assumptions were made [9]

- (a) The roll was considered a rigid body of the geometry as shown in the figure 4.
- (b) The material was assumed to be Mises material, which implies no strain hardening effect, no elastic deformation, and consequently, no volumetric change.
- (c) A kinematically admissible velocity field was assumed.
- (d) For the upper bound analysis, the contact surfaces between workpiece and roll were regarded as a surface of velocity discontinuity.

For the approximations assumptions made are:

- i. Constant shear stress between roll and strip.
- ii. Coulomb friction between die and strip i.e.

$$\text{Friction stress } \tau = \mu \sigma_0 \quad (4.1)$$

where σ_0 = stress normal to the die surface

μ = Coefficient of friction

Consider the figures 4, the die was divided into three zones. In zones I and III, the velocity is uniform and has only an axial component. In zone I the velocity is V_i , while in zone III the velocity is V_f and zone II is considered most vital zone where actual deformation is taking place.

A simple expression for the average roll pressure is given by Ref.19

$$P_{ave} = S_o \frac{e^{\mu L/t} - 1}{\mu L/t} \quad (4.2)$$

When no back and front tensions are applied, $S_o = (2/\sqrt{3})\sigma_o$. The thickness t is the average thickness of the strip, and L is the length of contact between the strip and rolls. Equation (4.2) is the result of assumption that the strip is forged in plane strain. Hessenberg's¹⁸ data show that the separation force is reduced about twice as effectively by back tension as it is by front tension. Introducing front and back tension effects on average pressure, Avitzur¹³ wrote in his eq. (28)

$$\frac{P_{avg}}{(2/\sqrt{3})\sigma_o} = \left[1 - \frac{1}{3} \frac{\sigma_{yf} + 2\sigma_{xb}}{(2/\sqrt{3})\sigma_o} \right] \frac{\exp(\mu L/t) - 1}{(\mu L/t)} \quad (4.3)$$

$$\text{where } t = \frac{1}{2}(t_o + t_f)$$

$$L = \sqrt{R_{RO}(t_o - t_f) + \left[\frac{8R_{RO}(1-\nu^2)}{\pi E} P_{avg} \right]^2} + \frac{8R_{RO}(1-\nu^2)}{\pi E} P_{avg} \quad (4.4)$$

For small and rigid rolls ($E \rightarrow \infty$) equation (4.4) converges to

$$L = \sqrt{R_{RO}(t_o - t_f)} \quad (4.5)$$

p_{avg} and L can be solved simultaneously by successive approximations. Initially, the approximation is made by assuming $p_{avg} = 0$ in eq. (4.4), which then converges to eq. (4.5). The computed L is inserted into eq. (4.3), and the first approximation for the average pressure is computed and then inserted into eq.

(4.4) for the computation of the second approximation of L , and so on. Usually, the solutions converge and any desired accuracy can be obtained.

4.2 LIMITING THICKNESS AND LIMITING REDUCTION:-

Sometimes the treatment of equations (4.3) and (4.4) does not yield a solution. Each consecutive step in solving equation (4.3), then (4.4) then (4.3) again, and so on, leads to larger and larger values of pressure and length of contact. This situation means that the limiting reduction or limiting thickness is reached. Any attempt to close the gap between the rolls results in higher pressure and further flattening of the rolls with increasing length of contact L , which in turn causes higher pressure, and so on. It means that one approaches both the limiting thickness and the limiting reduction with increasing roll diameter and reductions and with decreasing original thickness and modulus of the elasticity of the rolls E . The problem is important in rolling thin strip.

The thickness below the limiting thickness can be reduced by following methods:

- Reduce friction
- Reduce roll diameter
- Increase the rigidity of the roll material
- Apply higher front or back tensions
- Introduce hydrodynamic lubrication.

If the original strip thickness is slightly above the limiting thickness, the amount of reduction possible is limited by roll flattening. An attempt for too high a reduction will result in excessive pressure and roll flattening. Equations (4.3) and (4.4) will have no finite solution. If higher reductions are desired, the same changes are to be made as those suggested when limiting thickness was of concern. Large reductions can be obtained by the combination of small planetary rolls with a common large supporting roll.

The smaller the roll diameter, the smaller is the production rate because of lower velocity. When excessive pressure is the problem, four-high rolling mills are introduced to have the small area of contact through small working rolls supporting for rigidity against bending by the supporting rolls. The ratio of the working roll diameter to supporting roll diameter is no less than $\frac{1}{2}$. Smaller ratios will introduce bending in the horizontal plane. To overcome this, the cluster rolling mills were introduced to support very small diameter working rolls with a train of progressively increasing diameters of supporting rolls.

4.3 PROCESS VARIABLES:-

During the analysis of different defects found in rolling process, following variables are identified as the major causes of failure and whose manipulation leads to defectless product.

V_o = initial velocity

V_f = final velocity

σ_{xf} = front tension in case of extrusion

μ	=	coefficient of friction
α	=	semi die cone angle
L	=	Length of contact

In programming, zone II was divided into various grid point by using the equations:

$$r = r_f + \left(\frac{r_o - r_f}{n} \right) \quad \text{and} \quad \alpha = \theta/m . \quad (4.6)$$

By putting the value of 'm' and 'n' (m x n) grid points are located in die space and at these grid points the values of different strain rates are calculated . The values of strain rate s for the grid points are calculated on the basis of 'n' radial grid point for each value of ' α ' and 'm' angular grid points for each value of r. Together these generate (m x n) mesh. Corresponding to these grid points, different values of strain rate are plotted in the die space of zone II .

4.4 INTERMEDIATE DISTORTION ANALYSIS:-

A powerful tool for studying the flow pattern is visioplasticity. Analytically, the velocity field assumed can be used to predict the relative position of all points after deformation. The assumption made in the following equations is the constancy of volume. Any straight line parallel to the axis of symmetry at a distance R_1 , from the axis which is originally in the zone I, will end up in a product as straight line at the distance R obeying

$$\frac{R}{R_f} = \frac{R_1}{R_o} \quad (4.7)$$

A straight line perpendicular to the axis of symmetry and passing through the axis distorts during the deformation. This distortion is analyzed. The time to move this distance at the velocity V_o .

$$t_1 = R_o \left(\frac{1 - \cos \theta}{V_o \sin \alpha} \right) \quad (4.8)$$

where $R_f = t_f / 2$ and $R_o = t_o / 2$ where t_o = initial thickness of workpiece
 t_f = final thickness of rolled product

The time required for a point to move an incremental distance dr in zone II at the velocity v is

$$dt_2 = -\frac{dr}{v} = \frac{r^2 dr}{V_f r_f^2 \cos \theta} \quad (4.9)$$

By integration the time, the point takes to move from the boundary τ_2 to τ_1 is

$$t_2 = \frac{R_f / V_f}{3 \sin \alpha \cos \theta} \left[\left(\frac{R_o}{R_f} \right)^3 - 1 \right] \quad (4.10)$$

To cross the zone III, a point has to move an additional distance that takes time

$$t_3 = \frac{R_f}{V_f} \left(\frac{\cos \theta - \cos \alpha}{\sin \alpha} \right) \quad (4.11)$$

When the process is interrupted before completion, some grid lines are partially in zones I, II, and III. The shapes of the distorted grid lines in zone II are calculated in the computer program and shown in figures.

4.5 VELOCITY FIELD ANALYSIS:-

$$\dot{U}_r = \frac{V_f t_f}{R_o} \left(\frac{1}{t_f / R_o + \alpha_n^2} \right) \quad (4.12)$$

The above equation is used to develop the program because it is found that it is most suitable because it relates the die space variables r and θ with a number of process and material variables.

4.6 COMPUTATION OF VARIOUS PARAMETERS INVOLVED:-

A strip of initial radius R_o ($=t_o/2$) is pushed or pulled through rolls as in fig. (4). While passing through the rolls, the strip deforms plastically and decreases in diameter. The cylindrical portion of the rolls causes additional frictional losses, but it is required for the dimensional stability of the product of final radius R_f ($t_f/2$) and because of die manufacturing practice.

Due to volume constancy in zone II

$$V_o = \left(\frac{t_f}{t_o} \right) V_f \quad (4.13)$$

Strain rates obtained are

$$\dot{\epsilon}_R = -\dot{\epsilon}_\theta = 2 \left(\frac{t_f}{R_o^2} \right) \dot{U} \frac{\alpha}{(t_f/R_o + \alpha^2)^2} \quad (4.14)$$

All other $\dot{\epsilon}_{ij} = 0$

In zone II, the velocity is directed towards the apex (O of the cone). In the spherical coordinate system r, θ, ψ the velocity components are

$$\dot{U}_r = \frac{V_f t_f}{R_o} \left(\frac{1}{t_f/R_o + \alpha_n^2} \right) \quad (4.15)$$

$$U_\theta = U_\psi = 0$$

4.7 OPTIMAL ROLL RADIUS:-

With rolls of very small diameter, friction losses are reduced, but shear power is high. Too large a roll radius R_{RO} is associated with high friction losses.

The optimal roll radius is calculated as:-

$$\left(\frac{R_{RO}}{t_f}\right)_{opt} = \frac{1}{\left(m\left(\frac{t_o}{t_f} - 1\right)\right)} \quad (4.16)$$

4.8 DEAD ZONE FORMATION:-

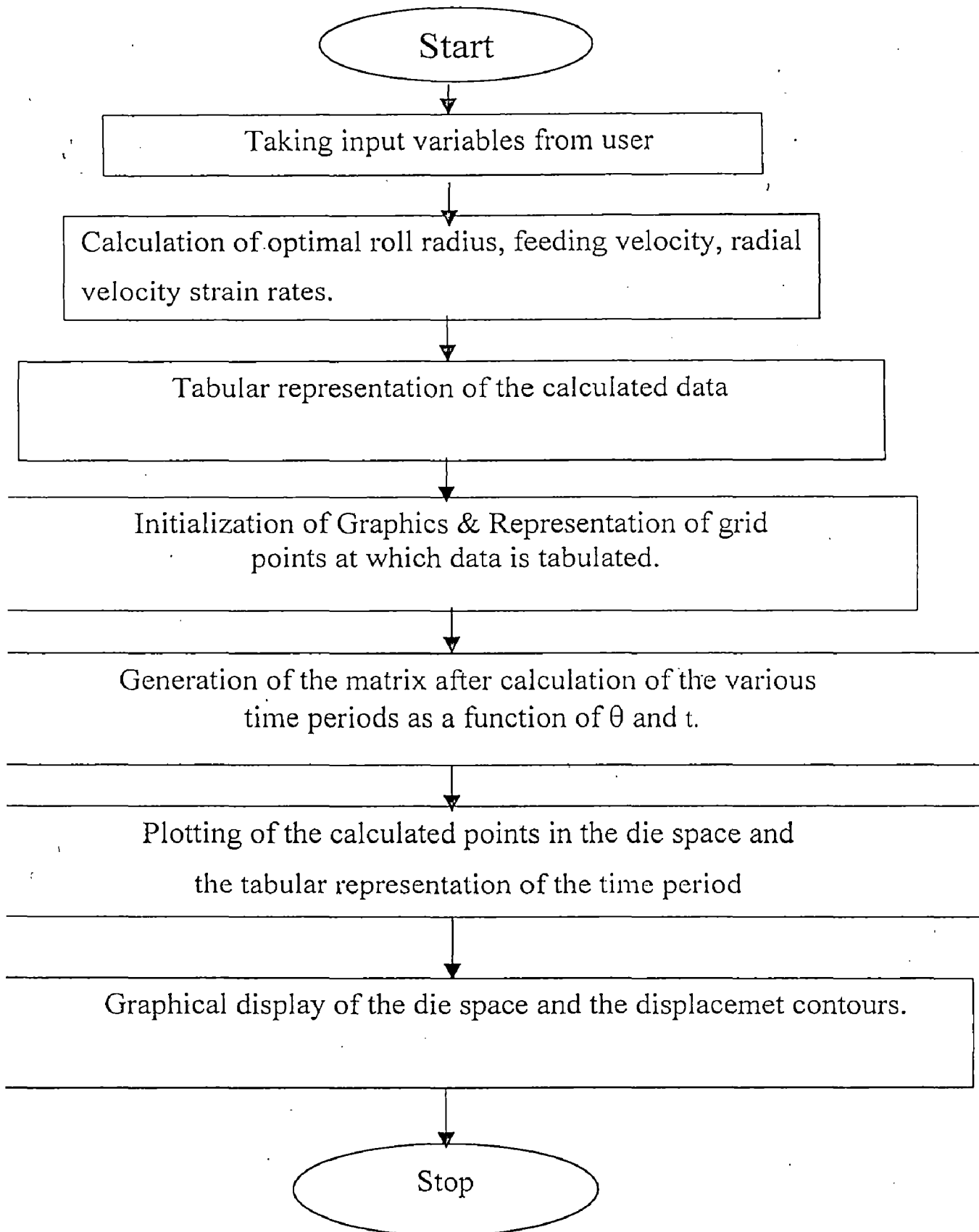
If the contact angle is too large, a dead zone is formed. The material adjoining the roll adheres to the rolls and is immobilized. A shear surface forms at a semi cone angle α_1 , the dead zone acts as a die like flow channel for the material. Friction between the dead-zone surface and the flowing material at α_1 , is no more than the value of the resistance of the material to shear (at α_r , is no more than the value of resistance of the material to shear ($\tau = \sigma_0/3$).

If the expected dead zone cone angle is small, it can be approximated similar to the optimal contact angle, and is given by

$$\alpha = [(3/2)m \ln (R_o/R_f)]^{1/2} \text{ (here } m=1) \quad (4.17)$$

α is defined as the critical contact angle, which causes dead zone formation. The critical contact angle is defined as the limiting angle, which causes dead-zone formation.

4.9 FLOW CHART OF THE PROGRAM



The results obtained are in the form of computer outputs. They are shown here after selecting the screen using Print Screen function and transferring the image into clipboard. The image of output is then retrieved from clipboard in the Paintbrush application software and modified to by inverting the colors. This gives the output in the form as shown in the given tables and figures.

The variables which ^{have been} identified are:

1. Reduction ratio
2. Contact angle
3. Shear factor
4. Roll radius

These variables takes care of the various possibilities that may arise during rolling.

The developed software is a simple treatment for rolling process and requires only few inputs that give us some interesting results. It is of vital interest that for any combination of process variables (other than roll radius) there exist a most suitable roll radius. With a roll of that radius $(R_{Roll})_{optimal}$ the required rolling load is at minimum. With roll of very small diameter, friction losses are reduced,

but shear power is high. Too large a roll radius is associated with high friction losses.

It is of interest to operate with such optimal roll radius that will minimize the necessary forces or in other words it will maximize possible reduction through rolling. This optimal roll radius is calculated through the software. For the calculation of rolling forces, material constant yield strength (σ_0) is required, which varies from material to material. Therefore depending upon the forces involved roll material varies.

1. As the friction increases, maximum possible reduction increases.
2. With roll of very small diameter, friction losses are reduced, but shear power is high. Too large a roll radius is associated with high friction losses. Therefore for any combination of process variables (other than roll radius), there exist a most suitable radius, $(R_{ROLL})_{opt}$.
3. Rolling is possible only because of friction. A minimum amount of friction is required for any reduction.
4. The waviness and residual stresses can be reduced by introducing front and back tension during rolling or by stretching slightly into the plastic range after rolling.
5. If the original strip thickness is only slightly above the limiting thickness, the amount of reduction possible is limited by roll flattening. An attempt for too high a reduction will result in excessive pressure and roll flattening.
6. As the reduction increases, contact angle increases. For a fixed roll radius, there exists an optimal contact angle that reduces rolling load.
7. As the friction factor becomes equal to one, dead zone formation occurs and the value of strain rate increases in a significant manner.

Chapter 7 **SUGGESTION FOR THE FUTURE WORK**

In the present work distorted grid pattern has been plotted in the die space taking time as variable. The displacement contours have been shown only for the deformation zone. The displacement profiles have been taken to be concave at the beginning, hence in future the adjacent zones can also be considered and a complete picture of flow pattern from the fed billet to end product can be obtained.

Further the present work is based on the analytical solution, instead Finite Element Method could be used to solve the differential equations by taking boundary conditions into consideration. Contouring of the various strain rates and velocity can be used for better speed and non-savable situations.

REFERENCES

1. DIETER GEOREG E., Mechanical metallurgy, 3rd edition, McGraw-Hill, pp.503-508, (1988)
2. AVITZUR B., Metal forming processes and analysis, TMH edition, pp. 153-214,(1977).
3. TMOMPSEN E.G., WOOD R.D.SAMUELSON A. and ZIENKIEWICZ O.C., Numiform 89,' Numerical methods in industrial processes, A.A.Balkema/Rolterdon/Brookfield, Netherland, (1989).
4. CHENOT J.L., and ONATE E., Modeling of metal forming processes, KLUVER academic Publishers, pp. 245-260,(May 1968).
5. YANG C.T., On the mechanics of wire drawing, Journal of engineering for industry, Trans ASME, pp. 523-530, (1968).
6. SHOBAIK A. H., THOMSEN E.G., A theoretical method for the analysis of metal working problems, Trans ASME, pp.343-352, (May 1968).
7. ROWE G.W., An introduction to the principles of metalworking, The Edward Arnold Ltd. U.K., pp.86-91, (1968).
8. HOUTFE VAN, AERNOUDT, SEVILLANO, GIL 3., LEFEVER, PAEMDONCK VAN, TAYLOR, On simulation of cyclic textures at the surfaces of drawn wires using a simple flow field model, Material sciences forum, Vol 157, No.2, pp.1881-1886, (1994).
9. AVITZUR B., Metal forming Processes and Analysis, TMH Edition , pp.436-490, 1977..

10. AVITZUR B., Tube sinking and expanding, Journal of engineering for industry, Trans ASME, pp.71-79, (1965).
11. AVITZUR B., Flow characteristics through conical converging dies, Trans ASME, Series B, Vol 88, No.4, pp.410-420, (1964).
12. HEARNE E.J., Mechanics of materials, Vol 2, 2nd edition, ButterworthHeinemann Ltd., pp. 749, (1995).
13. AVITZUR B., An upper bound approach to cold strip rolling, ASME Trans B, Engineering for industry, Vol 86, pp. 31-48, (1964).
14. SHABAIK A. and KOBAYASHI S., Computer application to the viscoplasticity method, Trans ASME, Series b, Journal of engineering for industry, Vol 89, pp.339-346, (1967).
15. LEOPOLD, JUERGEN, GUENTHER and HOLGER, Deformed lattice analyzing using neural networks, IEEE International conference on neural networks, pp.3094-3097.
16. GUPTA M.K., B.E. final year project report,'Development of computer program for extrusion', Department of metallurgy, University of Roorkee, 1998-1999.
17. ARORA P., B.E. final year project report,'Development of computer program for rolling', Department of metallurgy, University of Roorkee, 1997-1998.
18. W. C. F. Hesseberg: The Effect of Tension on Torque and Roll Force in Cold Strip Rolling, J. Iron Steel Inst. (LONDON), vol 168, pp.155-164, June, 1951.

```

#include<iostream.h>
#include<stdio.h>
#include<conio.h>
#include<math.h>
#include<graphics.h>
#include<iomanip.h>
#include <string.h>
int matherr (struct exception *a)
{
    if (a->type == DOMAIN)
        if (!strcmp(a->name,"sqrt")) {
            a->retval = sqrt (-(a->arg1));
            return 1;
        }
    return 0;
}
void main()
{
    int cn;
    double A,B;
    double to,ao,al,a,a2,alo,
    Ro,k,tf,z,mu,r,alp,vo,vf,ma[50][6],m,n,i,j,x,y,too,tff,mag,rr[50];
    double C,D;
    char ch,mesg[5];
    int maxx,maxy;
    start:
    clrscr();
    gotoxy(30,12);
    cout<<"Enter the initial thickness:";
    cin>>to;clrscr();
    gotoxy(30,12);
    cout<<"Enter the final thickness:";
    cin>>tf;clrscr();
    gotoxy(30,12);
    cout<<"Enter the final velocity:";
    cin>>vf;clrscr();
    gotoxy(30,12);
    cout<<"Enter the shear factor:";
    cin>>mu;clrscr();
    gotoxy(30,12);
    cout<<"Enter the griding factor:";
    cin>>m>>n;clrscr();
    gotoxy(30,12);
    cout<<"Do you want the program to deal with optimal roll radius (y/n)?:";
    cin>>ch;

```

```

if(ch=='y')
{
    Ro=tf/(mu *(to/tf-1));
    k=sqrt(tf/Ro);
    z=sqrt((to/tf)-1);
    ao=(1.0/3)*k* (atan(z)-(1.0/mu)*k*((log(to/tf))+(1.0/4)*(k*z)));
    gotoxy(30,12);
    cout<<"The value of optimal radius"<<setw(10)<<Ro<<endl;clrscr();
}
else
{
    gotoxy(30,12);
    cout<<"Enter the value of roll radius:";
    cin>>Ro;clrscr();
    z=sqrt((to/tf)-1);
    ao=(1.0/3)*(sqrt(tf/Ro)*(atan(z)-(1.0/mu)*sqrt(tf/Ro)*(log(to/tf)+(1.0/4)*
    sqrt(tf/Ro)*sqrt((to/tf)-1))));
    }
    al=ao*(180/22)*7;
    vo=(tf/to)*vf;
    gotoxy(30,12);
    cout<<"The value of feeding velocity is vo="<<setw(10)<<vo<<endl;clrscr();
    gotoxy(30,12);
    cout<<"The reduction ratio"<<setw(10)<<to/tf<<endl;clrscr();
    //cout<<"the alpha opitum angle is al="<<setw(10)<<al<<" degree"<<endl;
    gotoxy(30,12);
    cout<<"The optimum roll radius is"<<Ro<<endl;clrscr();
    a2=(sqrt(tf/Ro))*(sqrt((to/tf)-1));
    alo=a2*(180.0/22)*7;
    gotoxy(30,12);
    cout<<"Contact angle in strip rolling alo=";
    cout<<setw(10)<<alo<<" degree"<<endl;clrscr();
    A=270.00-alo;
    B=90.00+alo;
    C=180.00-alo;
    D=180.00+alo;
    cn=0;
    x=to/(2*sin(a2));
    y=tf/(2*sin(a2));
    too=to/(2*tan(a2));
    tff=tf/(2*tan(a2));
    a=Ro*sin(a2);
    cout<<"\n"<<setw(3)<<"S.No."<<setw(12)<<"angle"<<setw(13)<<"radius"<<
    setw(14)<<"veocity"<<setw(15)<<"er"<<setw(20)<<"et"<<endl;getche();
    for(i=0;i<m;i++)

```

```

{
    for(j=0;j<n;j++)
    {
        ma[cn][0]=(j+1)*a2/n;
        ma[cn][1]=x+((y-x)/m*i;
        ma[cn][2]=-vf*tf/to*1/(tf/to+ma[cn][0]*ma[cn][0]);
        ma[cn][3]=2*vf*tf/(Ro*Ro)*vf*ma[cn][0]*ma[cn][0]/(tf/Ro+ma[cn][0]*
            ma[cn][0])*(tf/Ro+ma[cn][0]*ma[cn][0]);
        ma[cn][4]=-ma[cn][3];
        cout<<setw(3)<<cn+1<<setw(12)<<ma[cn][0]*180*7/22<<setw(13)<<ma[cn]
            [1]<<setw(15)<<ma[cn][2]<<setw(15)<<ma[cn][3]<<setw(20)<<ma[cn][4]<<"\
            cn++;
        }
    }
    getch();
    begin:
        clrscr();
        gotoxy(30,12);
        cout<<"Enter the magnification number:";
        cin>>mag;getch();clrscr();
        int driver,mode;
        driver=DETECT;
        mode=DETECT;
        initgraph(&driver,&mode,"c:\\tc\\bgi");
        if((Ro+(tf/2))*mag<240)
        {
            clearviewport();
            clrscr();
            maxx=(getmaxx()/2)-140;
            maxy=getmaxy()/2;
            line(maxx,maxy,maxx+too*mag,maxy);
            line(maxx,maxy-(to/2)*mag,maxx-100,maxy-(to/2)*mag);
            line(maxx,maxy+(to/2)*mag,maxx-100,maxy+(to/2)*mag);
            line(maxx+a*mag,maxy-(tf/2)*mag,maxx+a*mag+100,maxy-
                (tf/2)*mag);

            line(maxx+a*mag,maxy+(tf/2)*mag,maxx+a*mag+100,maxy+(tf/2)*mag);
            arc(maxx+a*mag,maxy-(Ro+tf/2)*mag,A-30,300,Ro*mag);
            arc(maxx+a*mag,maxy+(Ro+tf/2)*mag,60,B+30,Ro*mag);
            setlinestyle(1,0,0);
            arc(maxx+too*mag,maxy,C,D,x*mag);
            arc(maxx+too*mag,maxy,C,D,y*mag);
            line(maxx,maxy-(to/2)*mag,maxx+too*mag,maxy);
            line(maxx,maxy+(to/2)*mag,maxx+too*mag,maxy);
            line(maxx-100,maxy,maxx+too*mag,maxy);
            line(maxx,maxy-(to/2)*mag,maxx+a*mag,maxy-(Ro+tf/2)*mag);

```

```

line(maxx+a*mag,maxy-(Ro+(tf/2))*mag,maxx+a*mag,maxy+(Ro+(tf/2))*mag);
line(maxx,maxy+(to/2)*mag,maxx+a*mag,maxy+(Ro+(tf/2))*mag);
    settxtjustify(1,2);getche();
    cn=0;
    for(i=0;i<m;i++)
        {
            for(int j=0;j<n;j++)
                {
                    rr[cn]=ma[cn][1]*mag;
                    sprintf(msg,"%d",cn+1);
                    outtextxy(maxx+too*mag-rr[cn]*cos(ma[cn][0]),maxy-rr[cn]*sin(ma[cn][0]),msg);
                    circle(maxx+too*mag-rr[cn]*cos(ma[cn][0]),maxy-rr[cn]*sin(ma[cn][0]),1);
                    circle(maxx+too*mag-rr[cn]*cos(ma[cn][0]),maxy+rr[cn]*sin(ma[cn][0]),1);
                    cn++; getche();
                }
        }
    }
else
if(((Ro+(tf/2))*mag>=240) && (too*mag<478))
{

    clearviewport();
    maxx=getmaxx()/2-140;
    maxy=getmaxy()/2;
    line(maxx,maxy,maxx+too*mag,maxy);
    line(maxx,maxy-(to/2)*mag,maxx-50,maxy-(to/2)*mag);
    line(maxx,maxy+(to/2)*mag,maxx-50,maxy+(to/2)*mag);
    line(maxx+(too-tff)*mag,maxy-(tf/2)*mag,maxx+(too-tff)*mag+100,maxy-(tf/2)*mag);
line(maxx+(too-tff)*mag,maxy+(tf/2)*mag,maxx+(too-tff)*mag+100,maxy+(tf/2)*mag);
    line(maxx,maxy-(to/2)*mag,maxx+(too-tff)*mag,maxy-(tf/2)*mag);
    line(maxx,maxy+(to/2)*mag,maxx+(too-tff)*mag,maxy+(tf/2)*mag);
    setlinestyle(1,0,0);
    line(maxx-50,maxy,maxx,maxy);
    line(maxx+too*mag,maxy-(tf/2)*mag,maxx+too*mag,maxy+(tf/2)*mag);
    line(maxx,maxy-(to/2)*mag,maxx+too*mag,maxy);
    line(maxx,maxy+(to/2)*mag,maxx+too*mag,maxy);
    line(maxx+too*mag,maxy-(tf/2)*mag,maxx+too*mag,maxy+(tf/2)*mag);
    arc(maxx+too*mag,maxy,C,D,x);
    settxtjustify(1,2); getche();
    cn=0;
    for(i=0;i<m;i++)
        {
            for(int j=0;j<n;j++)

```

```

        {
            rr[cn]=ma[cn][1]*mag;
            sprintf(mesg,"%d",cn+1);
            outtextxy(maxx+too*mag-rr[cn]*cos(ma[cn][0]),maxy-rr[cn]*sin(ma[cn][0]),mesg);
            circle(maxx+too*mag-rr[cn]*cos(ma[cn][0]),maxy-rr[cn]*sin(ma[cn][0]),1);
            circle(maxx+too*mag-rr[cn]*cos(ma[cn][0]),maxy+rr[cn]*sin(ma[cn][0]),1);
            cn++;getche();
        }
    }
    else if(too*mag>478)
    {
        gotoxy(30,12);
        cout<<"Graphic output is spreading beyond the screen.";
        gotoxy(30,13);
        cout<<"Reduce the magnification number.";
        gotoxy(36,14);
        cout<<"Press any key...";cin>>ch;
        //clrscr();
        goto begin;
    }
    clrscr();

    cout<<setw(3)<<"S. No."<<setw(10)<<"angle"<<setw(13)<<"t1"<<
    setw(10)<<"t2"<<setw(12)<<"t3"<<setw(13)<<"t4 " <<endl;getche();
    double gr[20][4];
    for(i=0;i<20;i++)
    {
        gr[i][0]=(a2/20)*(i+1);
        gr[i][1]=(to/2)*(1-cos(gr[i][0]))/((sin(a2)*vo));
        gr[i][2]=(tf/vf)/(6*sin(a2)*cos(gr[i][0]))*(pow((to/2),3.0)-1);
        gr[i][3]=(tf/2*vf)*(cos(gr[i][0])-cos(a2))/sin(a2);
        gr[i][4]=gr[i][1]+gr[i][2]+gr[i][3];
        cout<<setw(3)<<i+1<<setw(11)<<gr[i][0]*180*7/22<<setw(14)<<gr[i][1]
        <<setw(12)<<gr[i][2]<<setw(13)<<gr[i][3]<<setw(13)<<gr[i][4]<<"\n";
    }getche();

    clearviewport();
    getche();
    maxx=(getmaxx()/2)-140;
    maxy=getmaxy()/2;
    line(maxy,maxy,maxx+too*mag,maxy);
    line(maxx,maxy+(to/2)*mag,maxx+(too-tff)*mag,maxy+(tf/2)*mag);
    line(maxx,maxy-(to/2)*mag,maxx+(too-tff)*mag,maxy-(tf/2)*mag);

```

```

line(maxx,maxy,maxx+too*mag,maxy);
line(maxx+(too-tff)*mag,maxy-(tf/2)*mag,(maxx+(too-tff)*mag+100),maxy-
(tf/2)*mag);
line(maxx+(too-tff)*mag,maxy+(tf/2)*mag,(maxx+(too-
tff)*mag+100),maxy+(tf/2)*mag);
setlinestyle(1,0,0);
line(maxx,(maxy-(to/2)*mag),(maxx+(too*mag)),maxy);
line(maxx,(maxy+(to/2)*mag),(maxx+(too*mag)),maxy);
setlinestyle(3,0,0);
line(maxx,(maxy-(to/2)*mag),maxx,(maxy+(to/2)*mag));
// line((maxx-(to/2)*mag),maxy,(maxx-(to/2)*mag/2),maxy);
line((maxx+too*mag),(maxy-60),(maxx+too*mag),(maxy+60));
settextjustify(1,2);
double pt[50][3],theta;
setlinestyle(3,1,0);
for(i=0;i<3;i++)
{
    z=(tff*mag/8)*(i+1);
    x=maxx-z;
    for(j=0;j<50;j++)
    {
        line(x,(maxy-(to/2)*mag),x,(maxy+(to/2)*mag));
    }
}
for(i=0;i<9;i++)
{
    pt[i][0]=(gr[1][2]/10)*(i);

    for(j=0;j<10;j++)

    {
        pt[j][1]=a2/1*(j+1);
        x=pt[i][0]*(3*vf*(pow(tf/(2*sin(a2)),2.0))*cos(pt[j][1]));
        y=pow((to/(2*sin(a2))),3.0);
        pt[i][2]=pow((y-x),1.0/3.0);
        circle(maxx+too*mag-mag*pt[i][2]*cos(pt[j][1]),maxy-
mag*pt[i][2]*sin(pt[j][1]),1);
        circle(maxx+too*mag-
mag*pt[i][2]*cos(pt[j][1]),maxy+mag*pt[i][2]*sin(pt[j][1]),1);
    }
}
getch();
closegraph();
clrscr();

```

```
cout<<"Do you want to see the graphics part again at different  
magnification "<<endl;  
cin>>ch;  
if(ch=='y') goto begin;  
cout<<"do you want to check more values?"<<endl;  
cin>>ch;  
    if (ch=='y') goto start;  
  
}
```

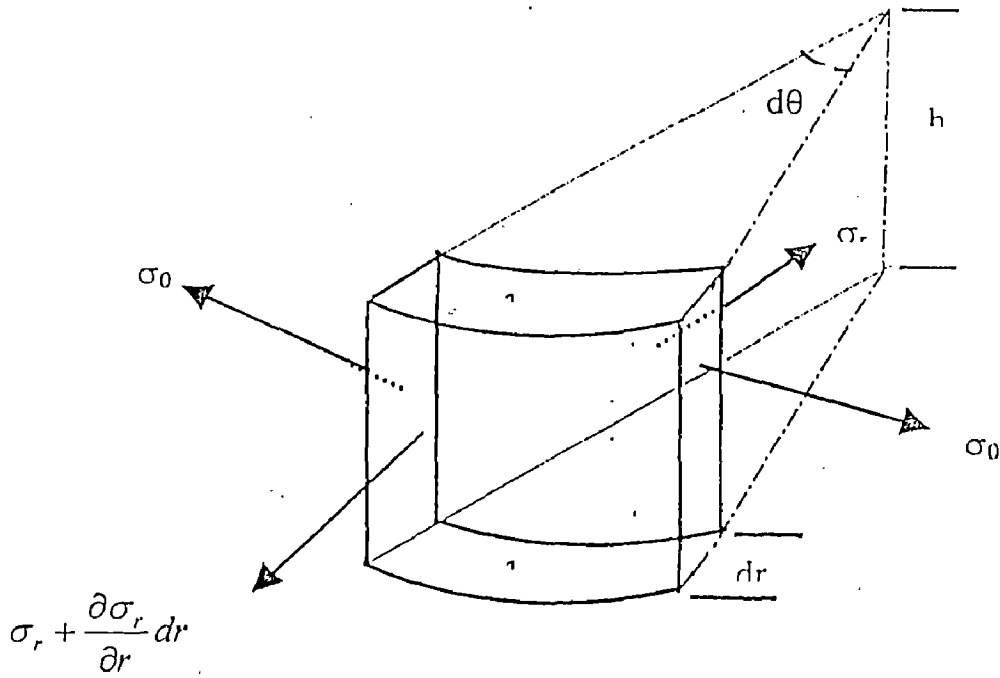



Fig.1 An Element in Axisymmetric Equilibrium Analysis

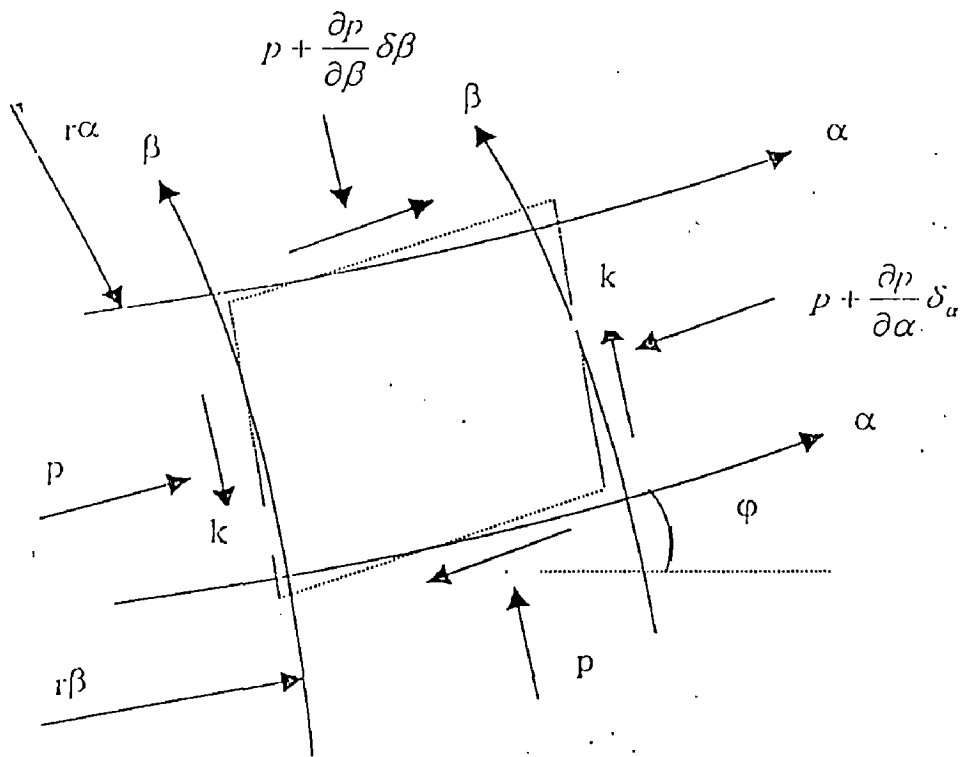


Fig.2 AN ELEMENT BETWEEN α AND β SLIP LINE

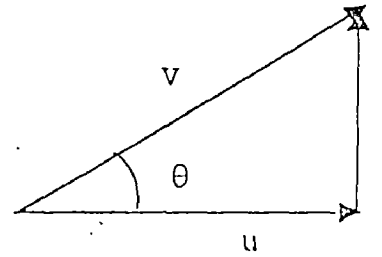
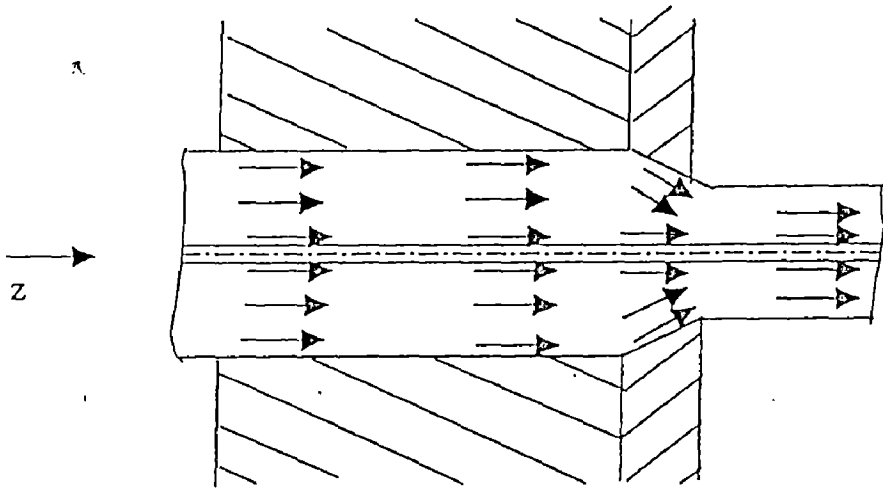
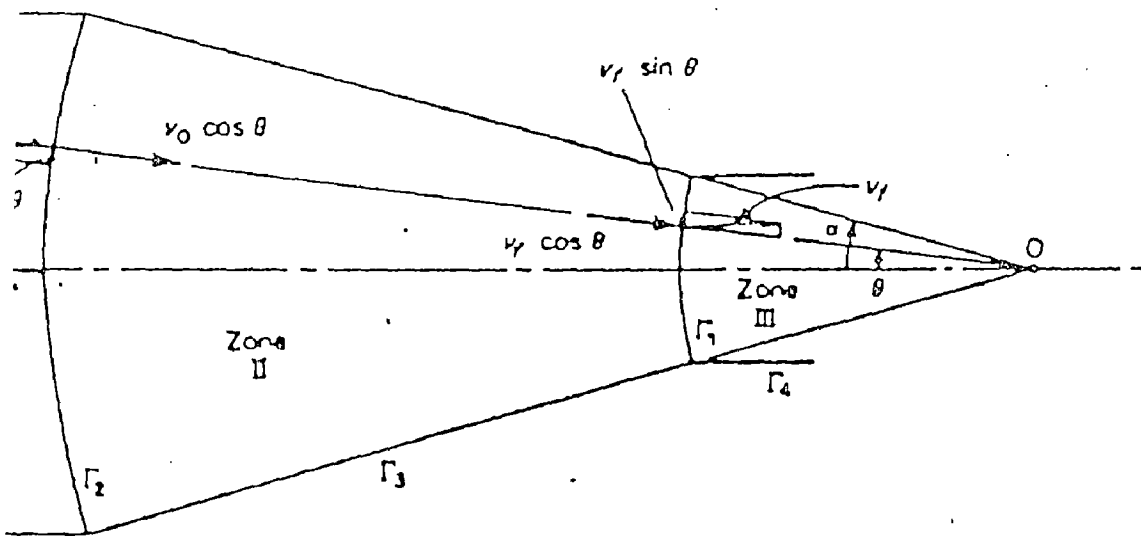


Fig. 3. Diagrammatic particle velocity field in tube extrusion



4 Velocity field.

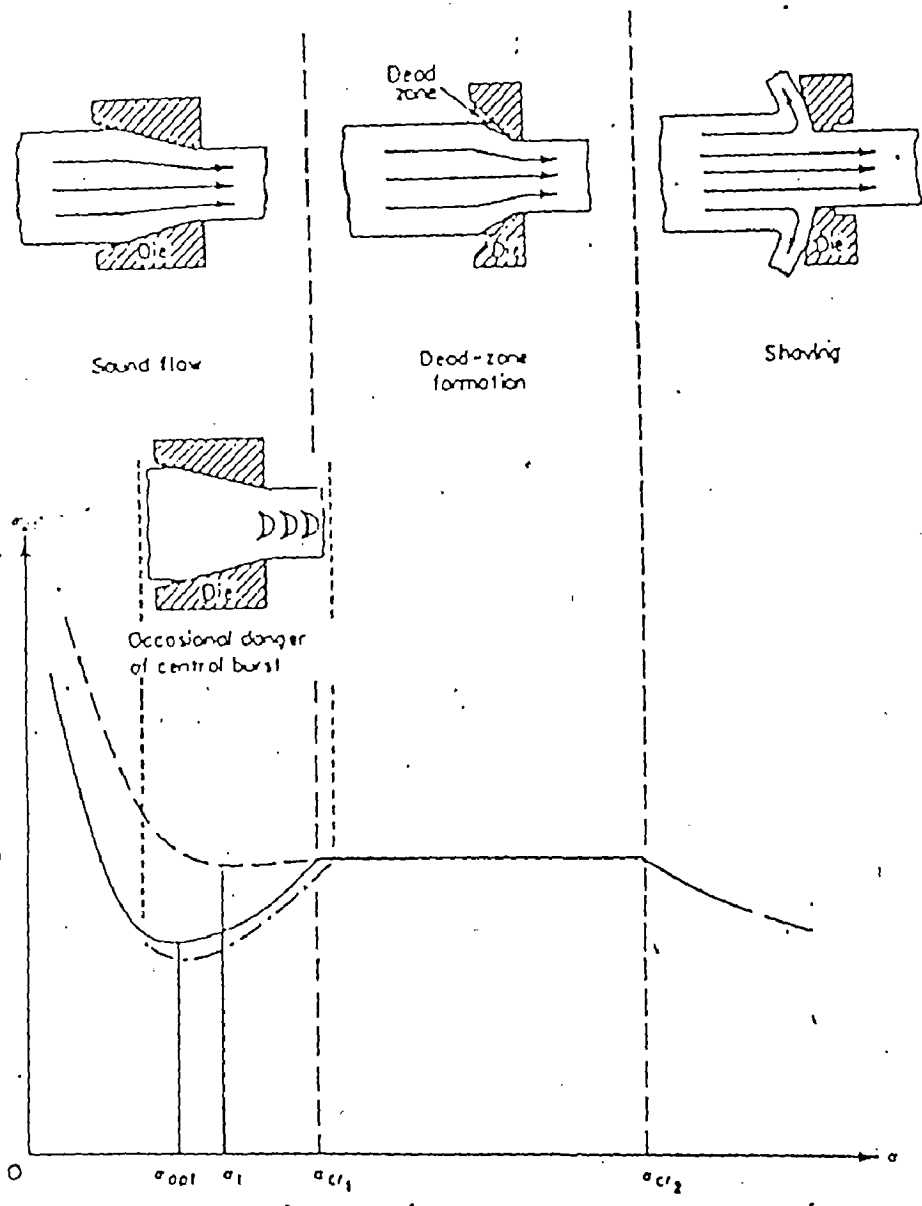


Fig.5(.) Drawing stress as a function of die semi-cone angle.

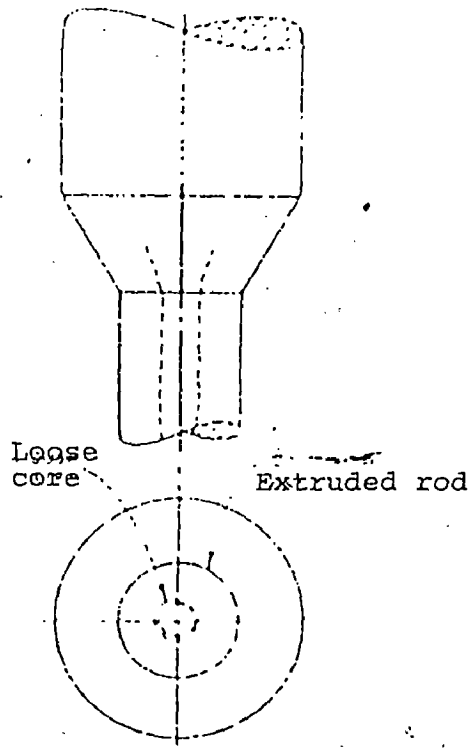


Fig. 6(a) Loose core

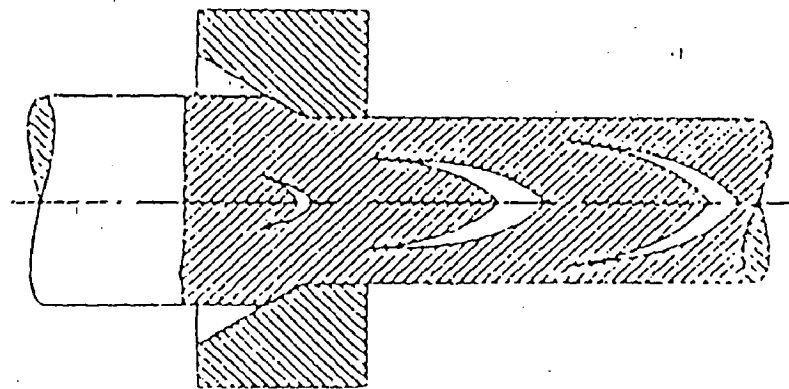
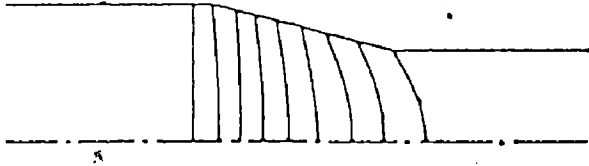


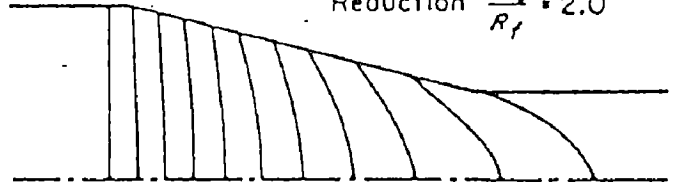
Fig 6(b) Central bursting.

Cone angle $\alpha = 15^\circ$
Reduction $\frac{R_0}{R_f} = 1.5$



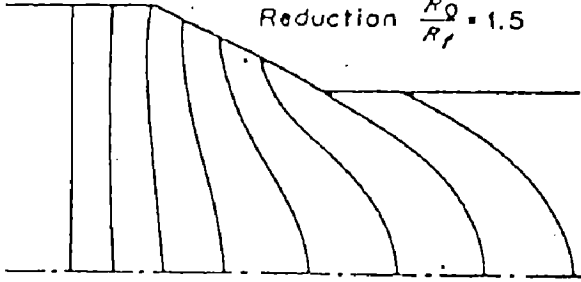
(a)

Cone angle $\alpha = 15^\circ$
Reduction $\frac{R_0}{R_f} = 2.0$



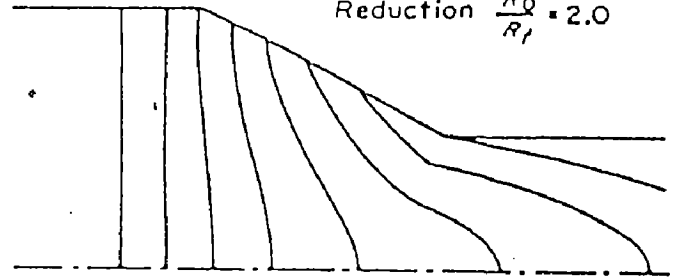
(b)

Cone angle $\alpha = 30^\circ$
Reduction $\frac{R_0}{R_f} = 1.5$



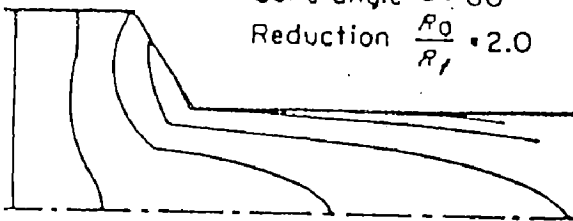
(c)

Cone angle $\alpha = 30^\circ$
Reduction $\frac{R_0}{R_f} = 2.0$



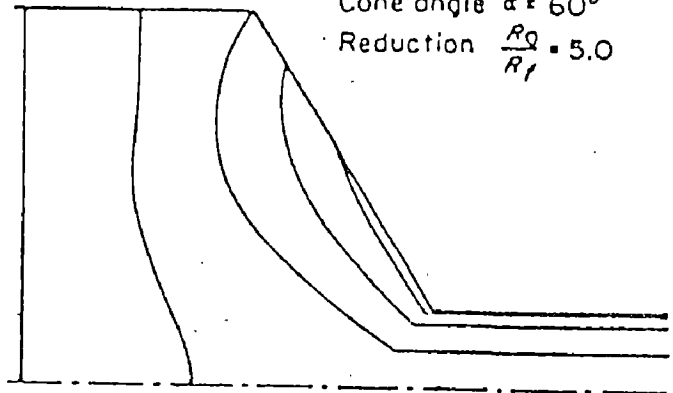
(d)

Cone angle $\alpha = 60^\circ$
Reduction $\frac{R_0}{R_f} = 2.0$



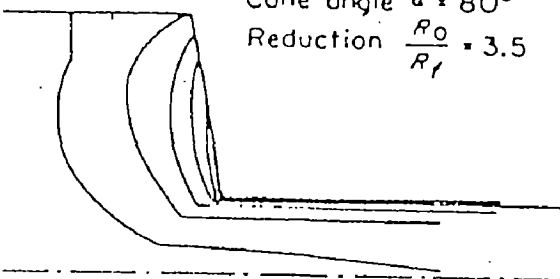
(e)

Cone angle $\alpha = 60^\circ$
Reduction $\frac{R_0}{R_f} = 5.0$



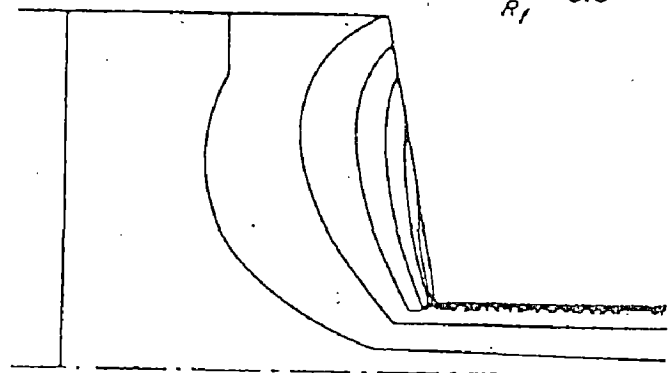
(f)

Cone angle $\alpha = 80^\circ$
Reduction $\frac{R_0}{R_f} = 3.5$



(g)

Cone angle $\alpha = 80^\circ$
Reduction $\frac{R_0}{R_f} = 5.0$



(h)

Intermediate grid deformation pattern.

510553.



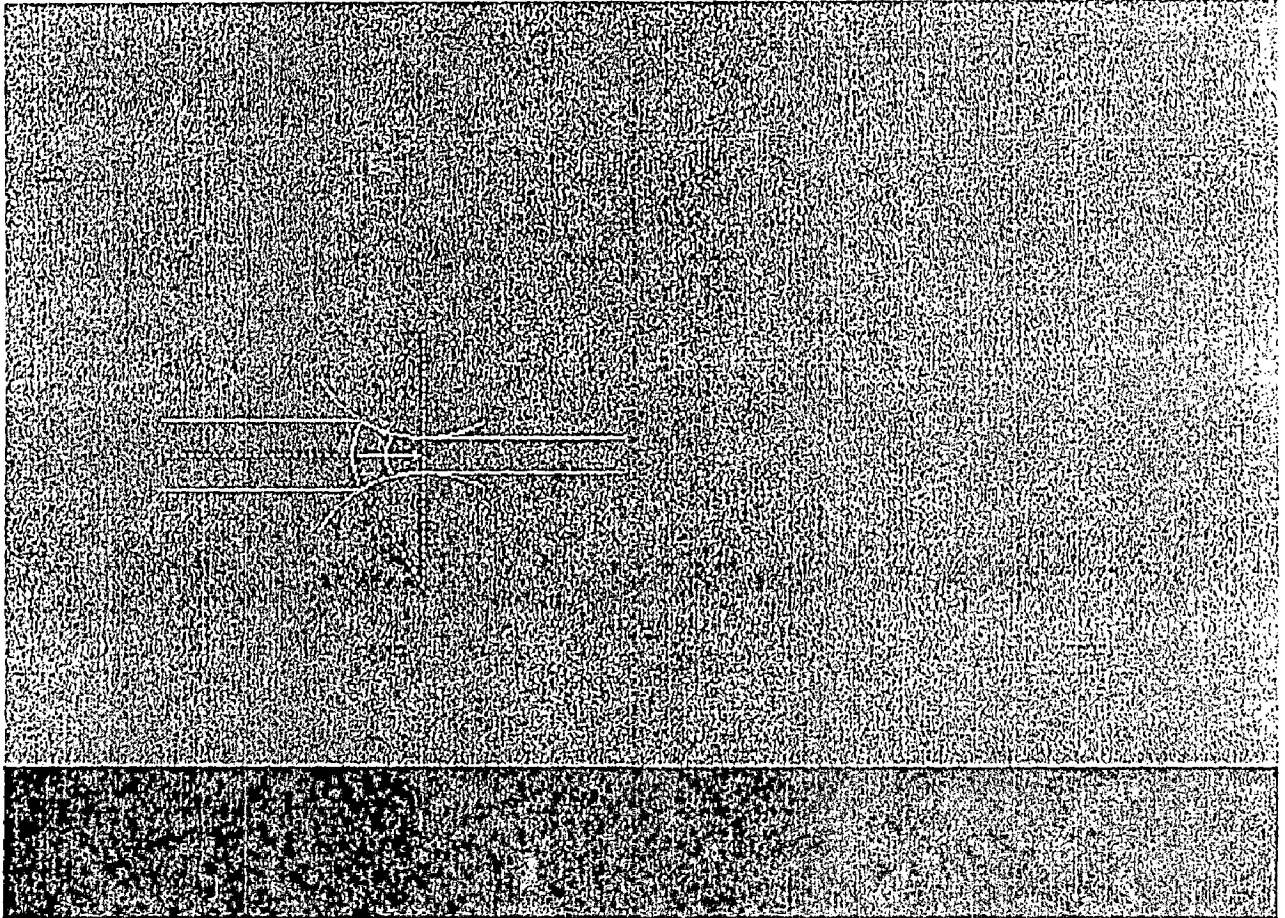


Fig. 8

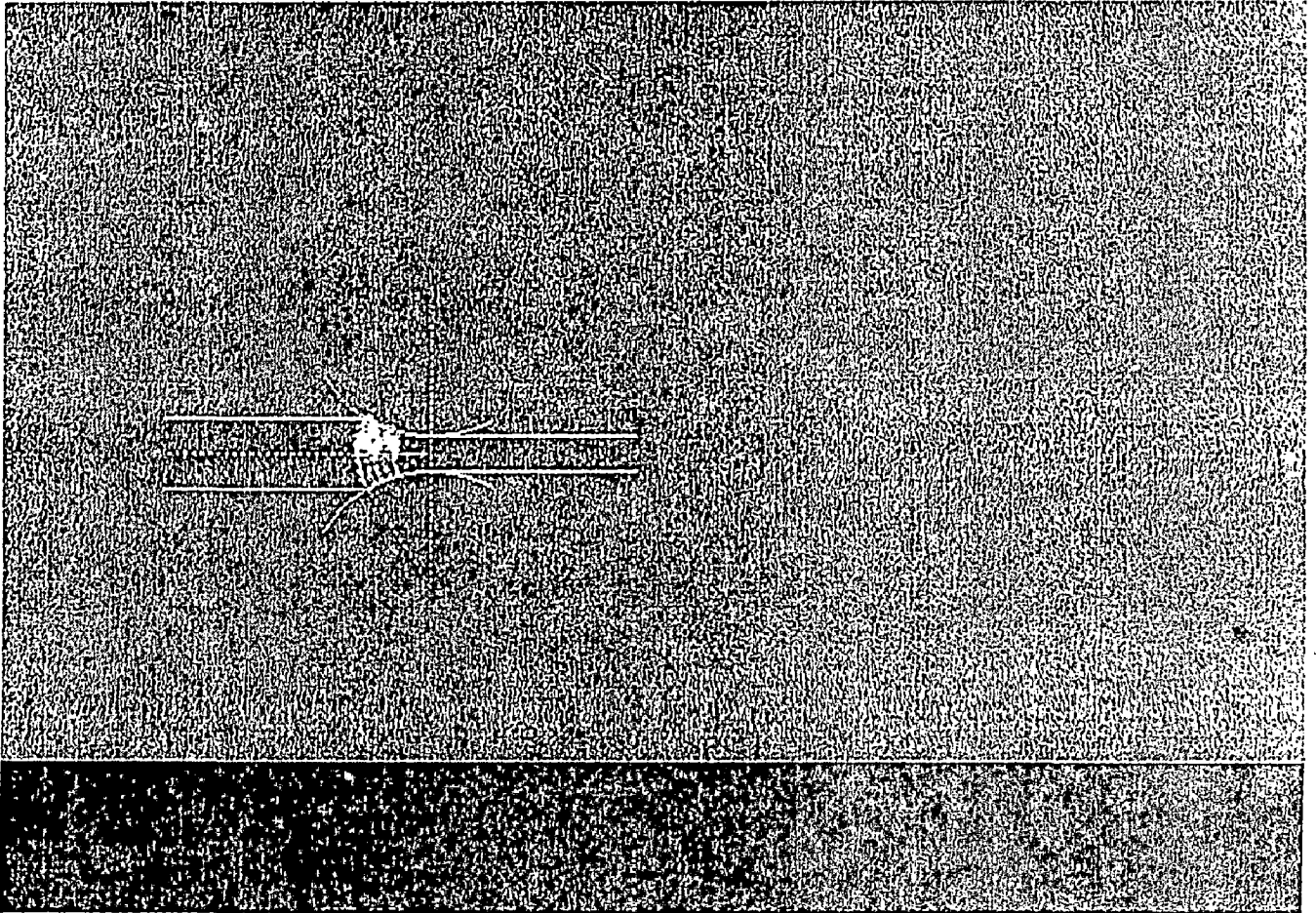


Fig. 9

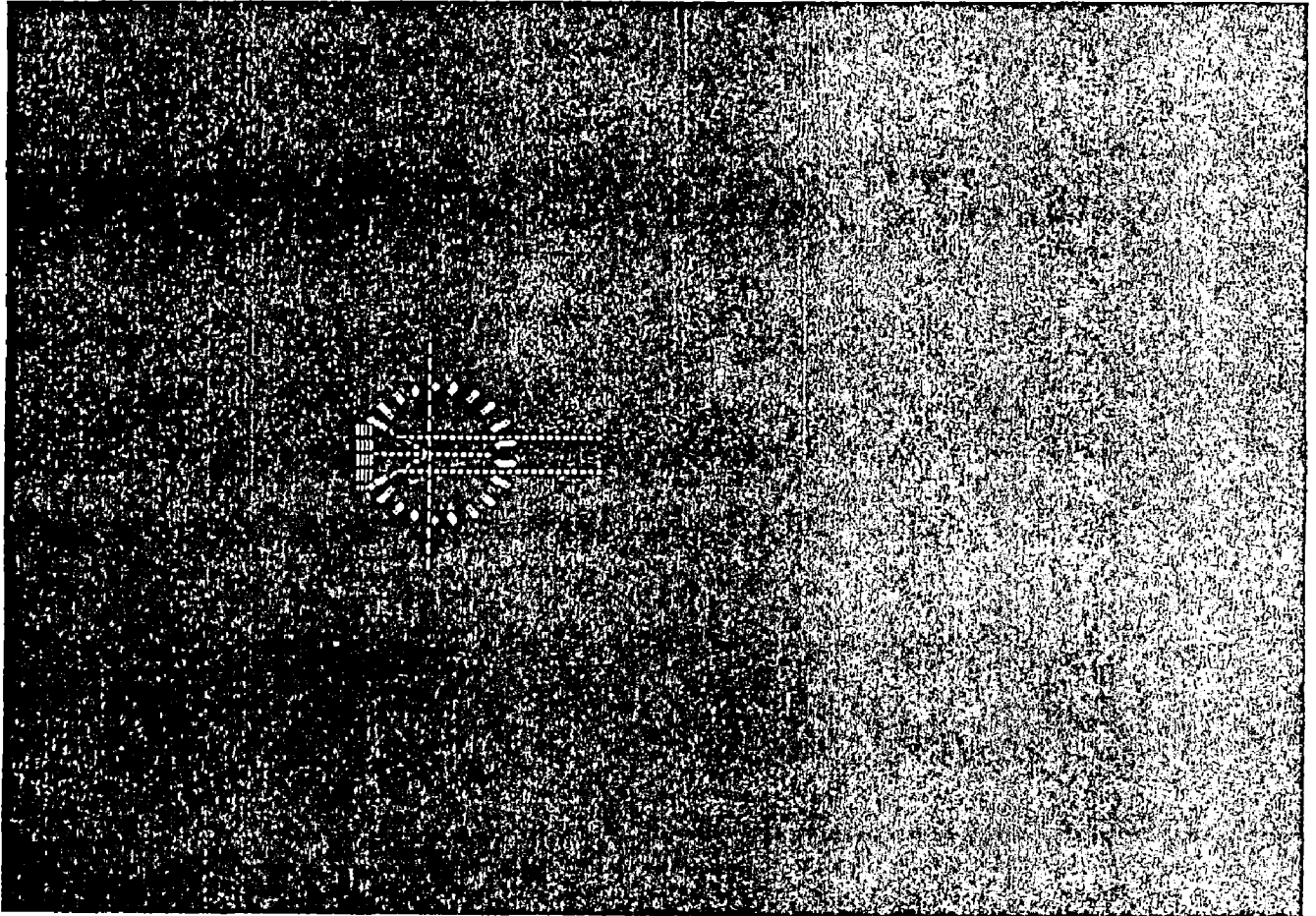


Fig. 10

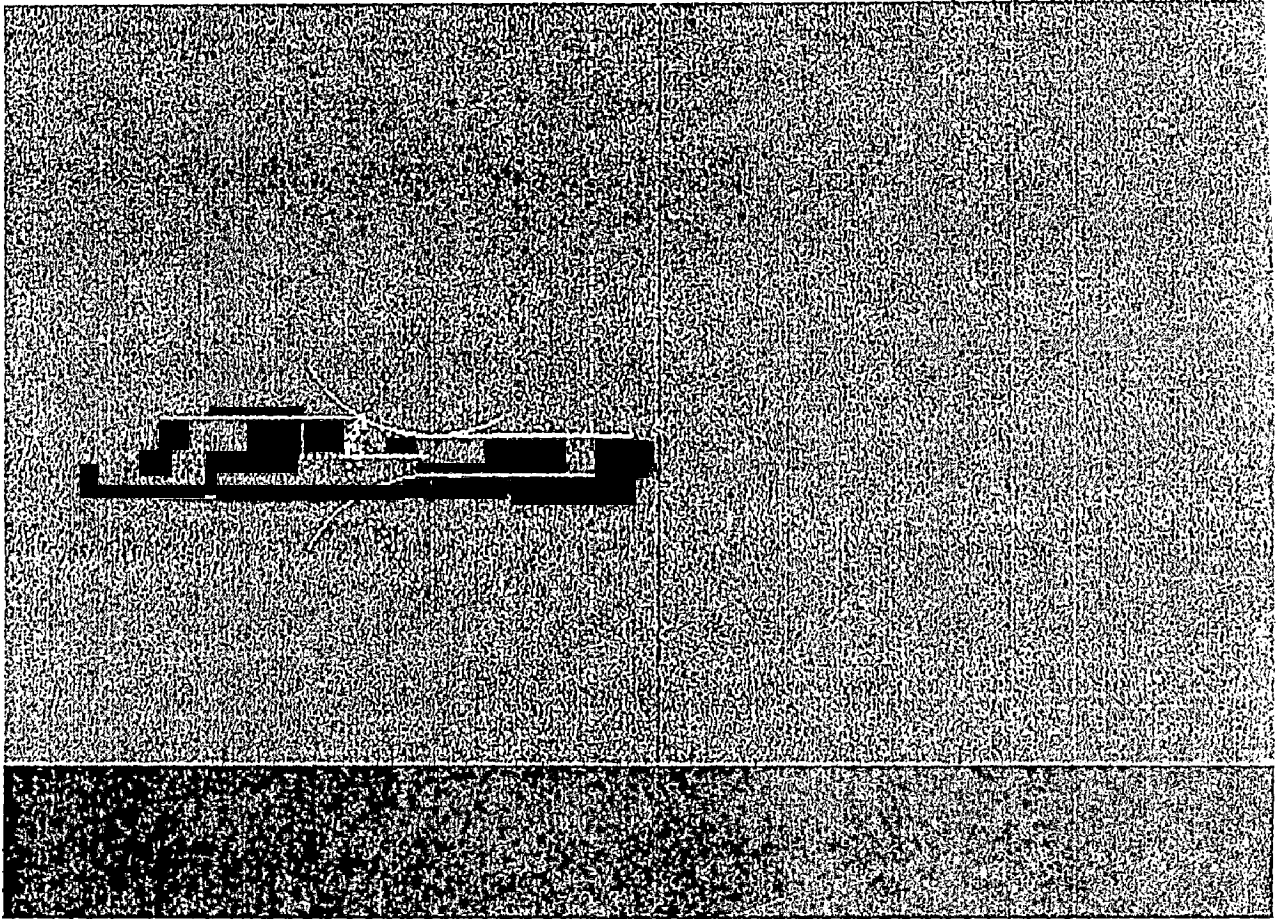


Fig. 12

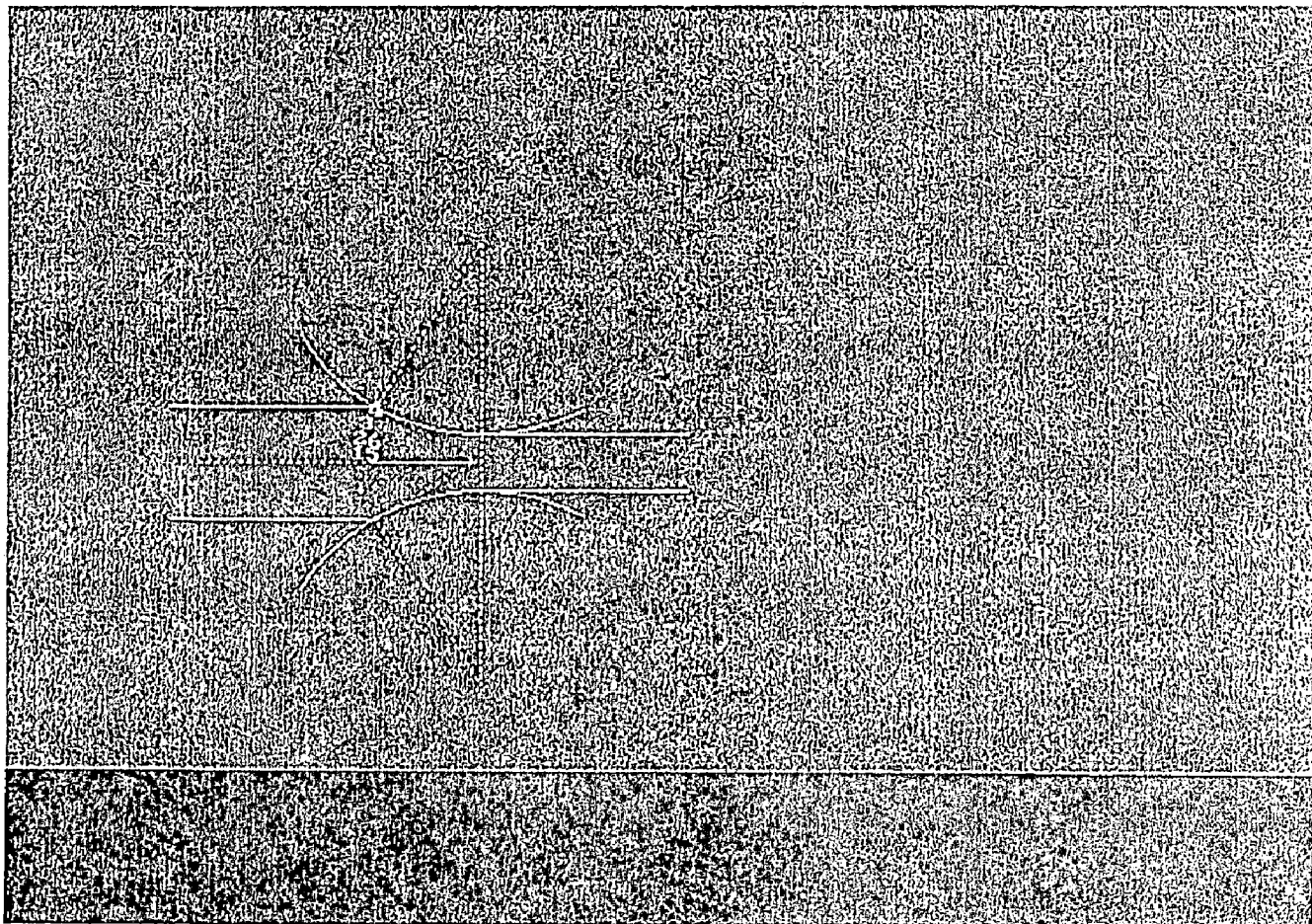


Fig. 13

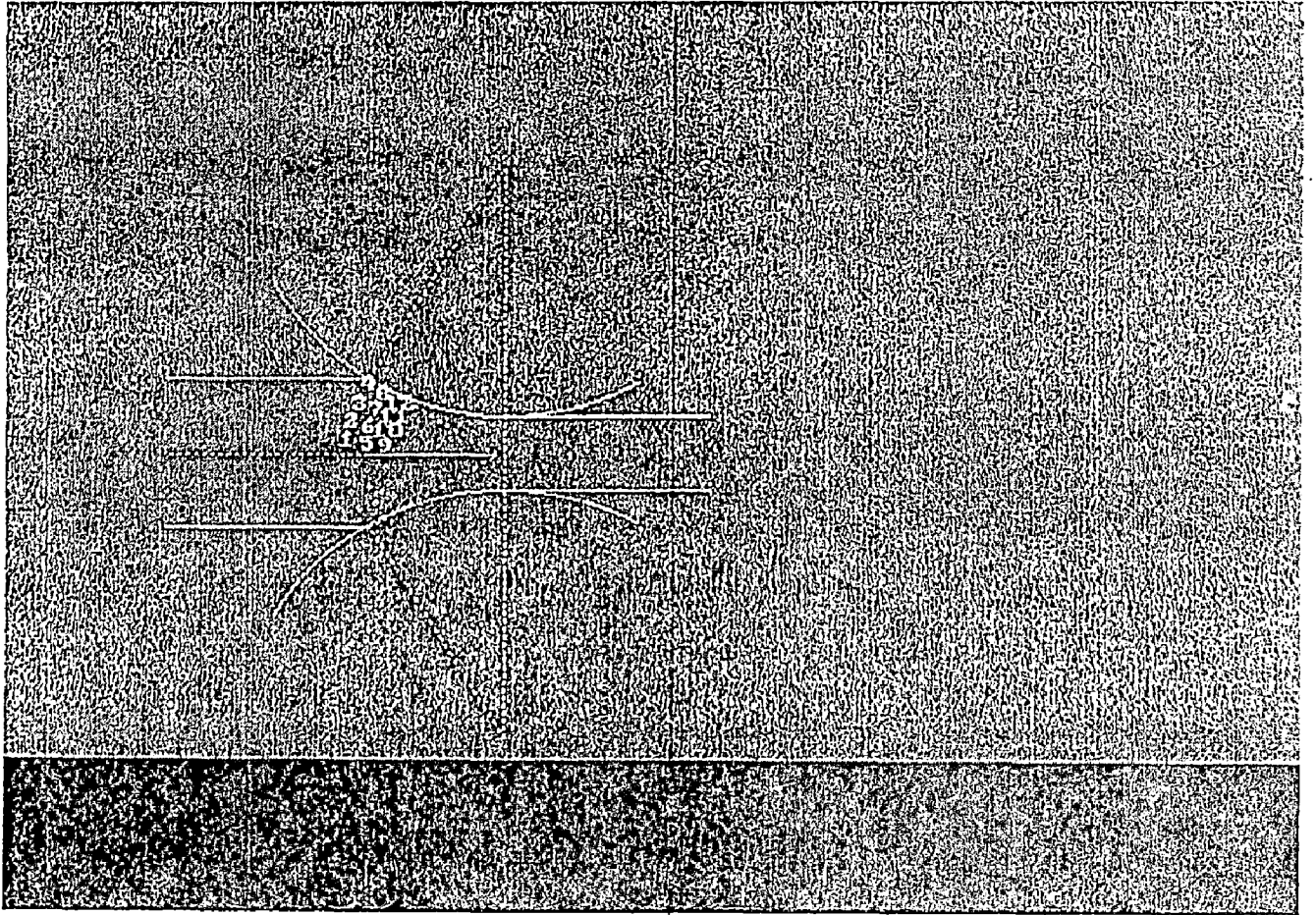


Fig. 14

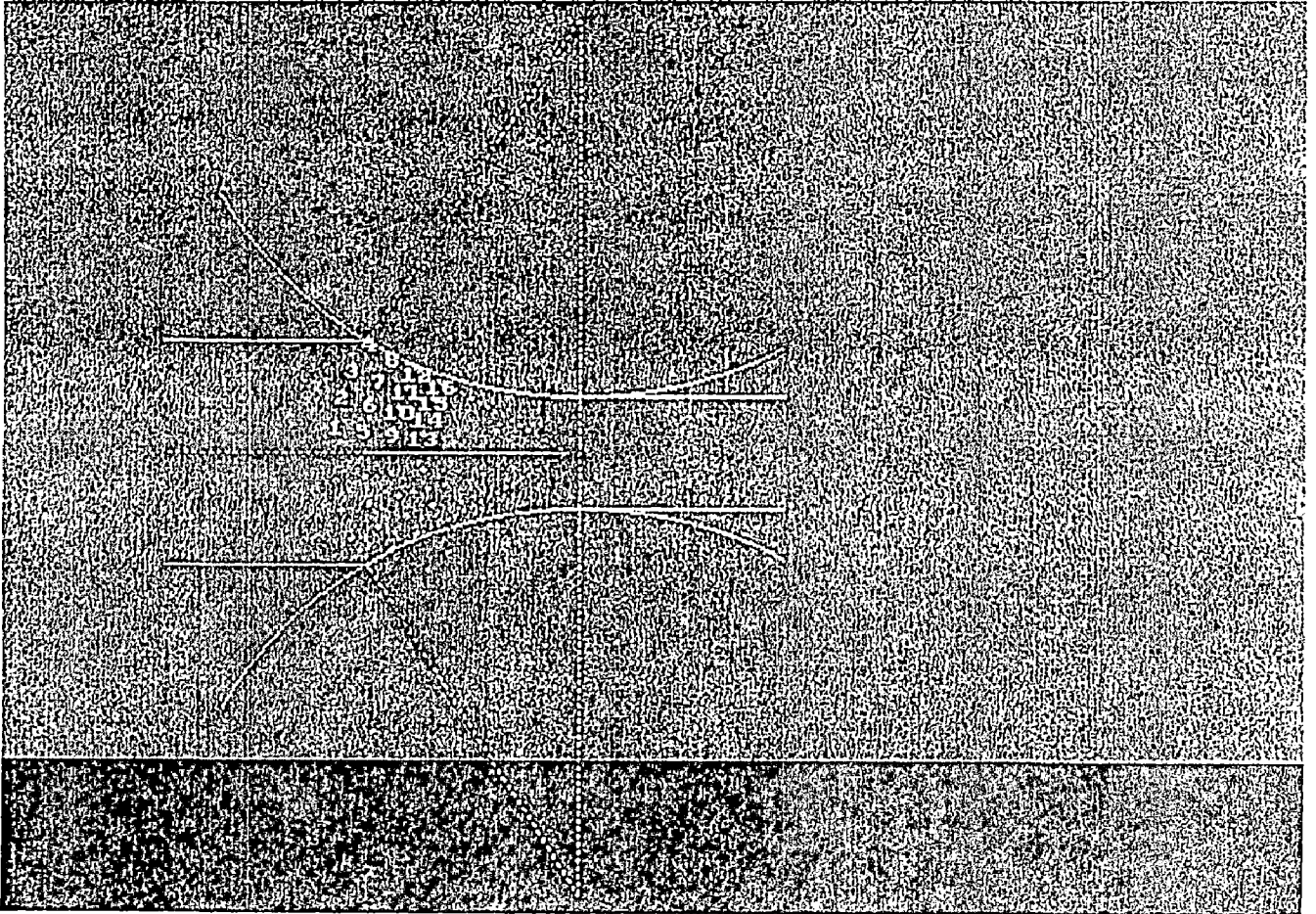


Fig.15

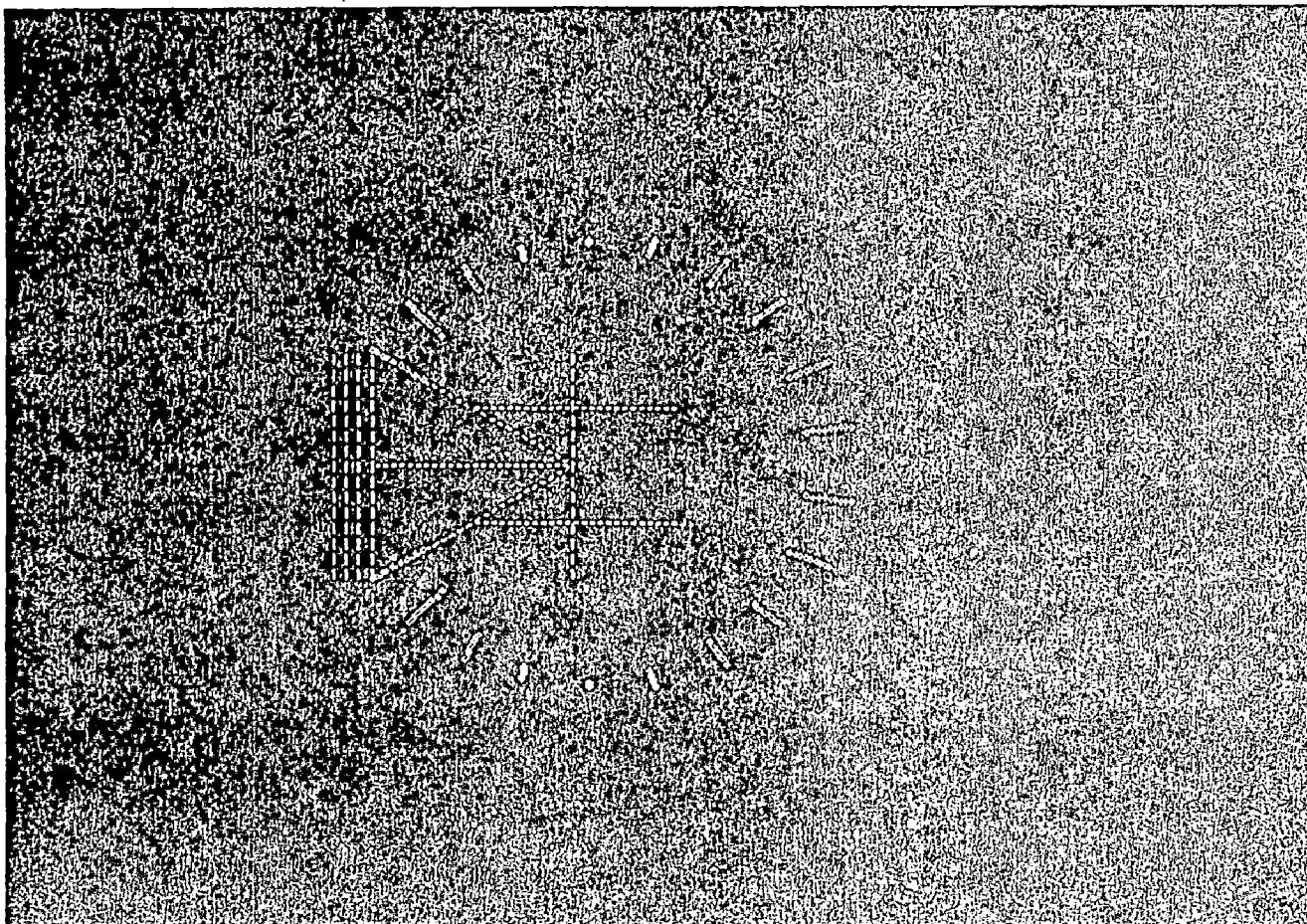


Fig.16

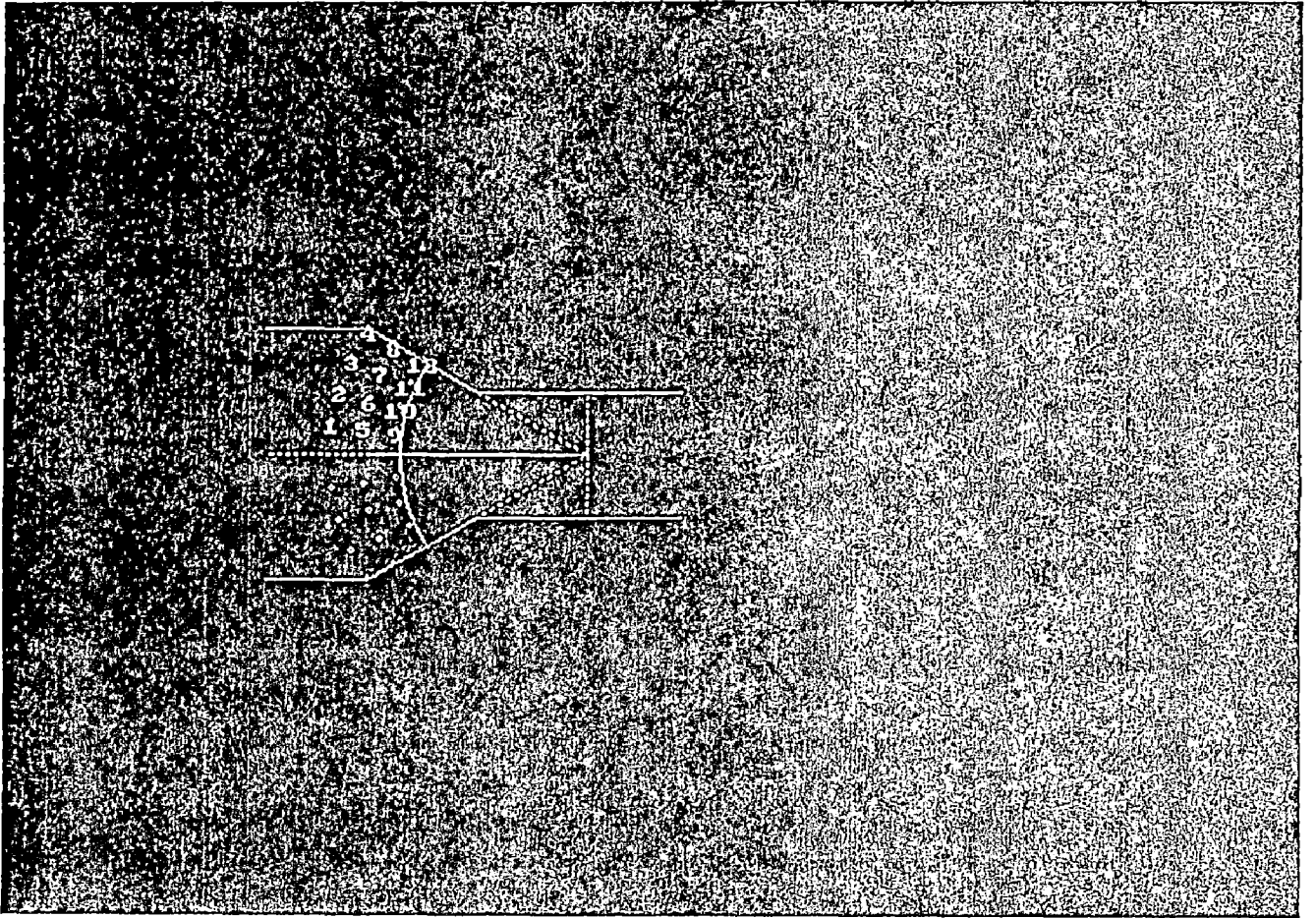


Fig.17

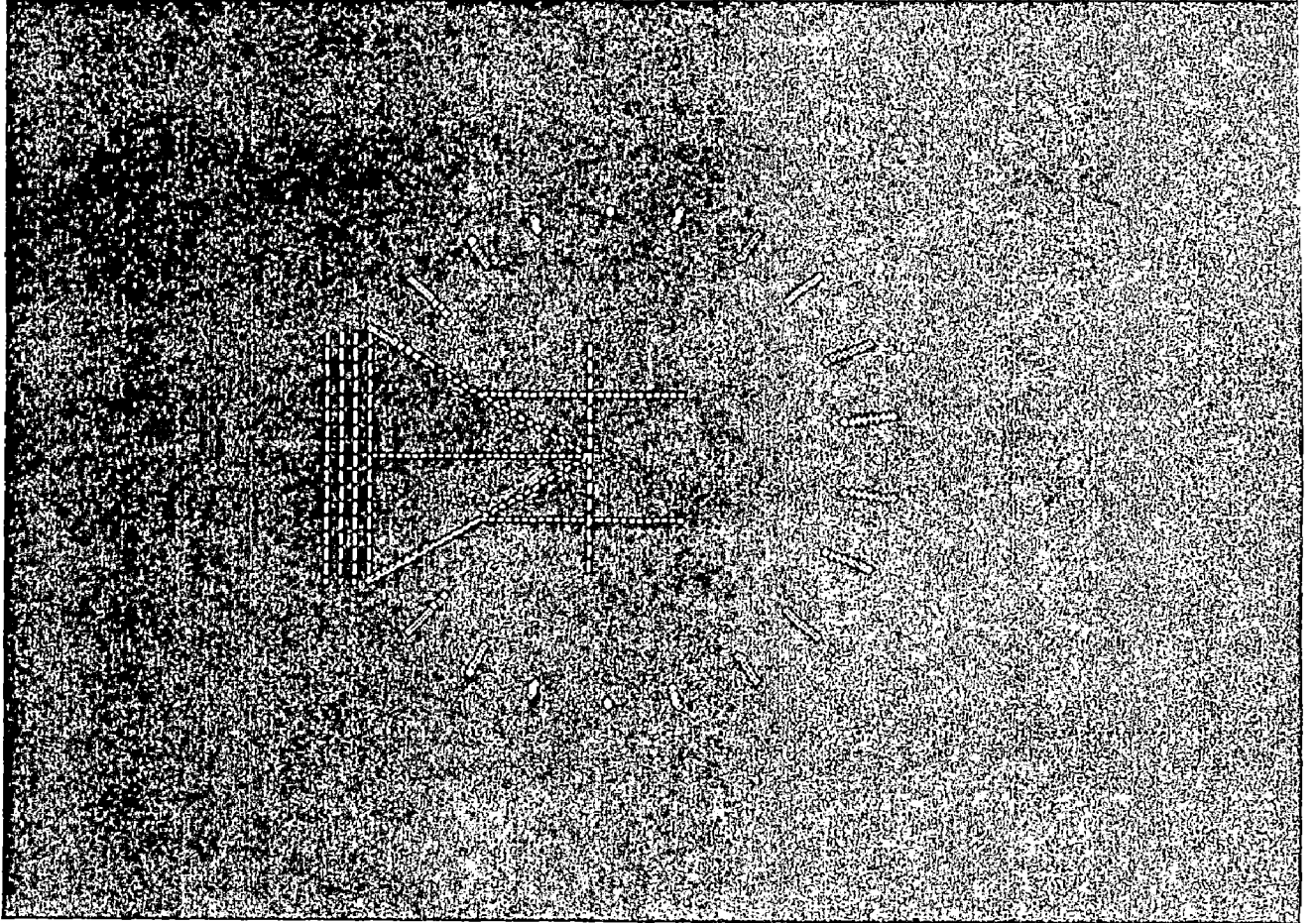


Fig.18

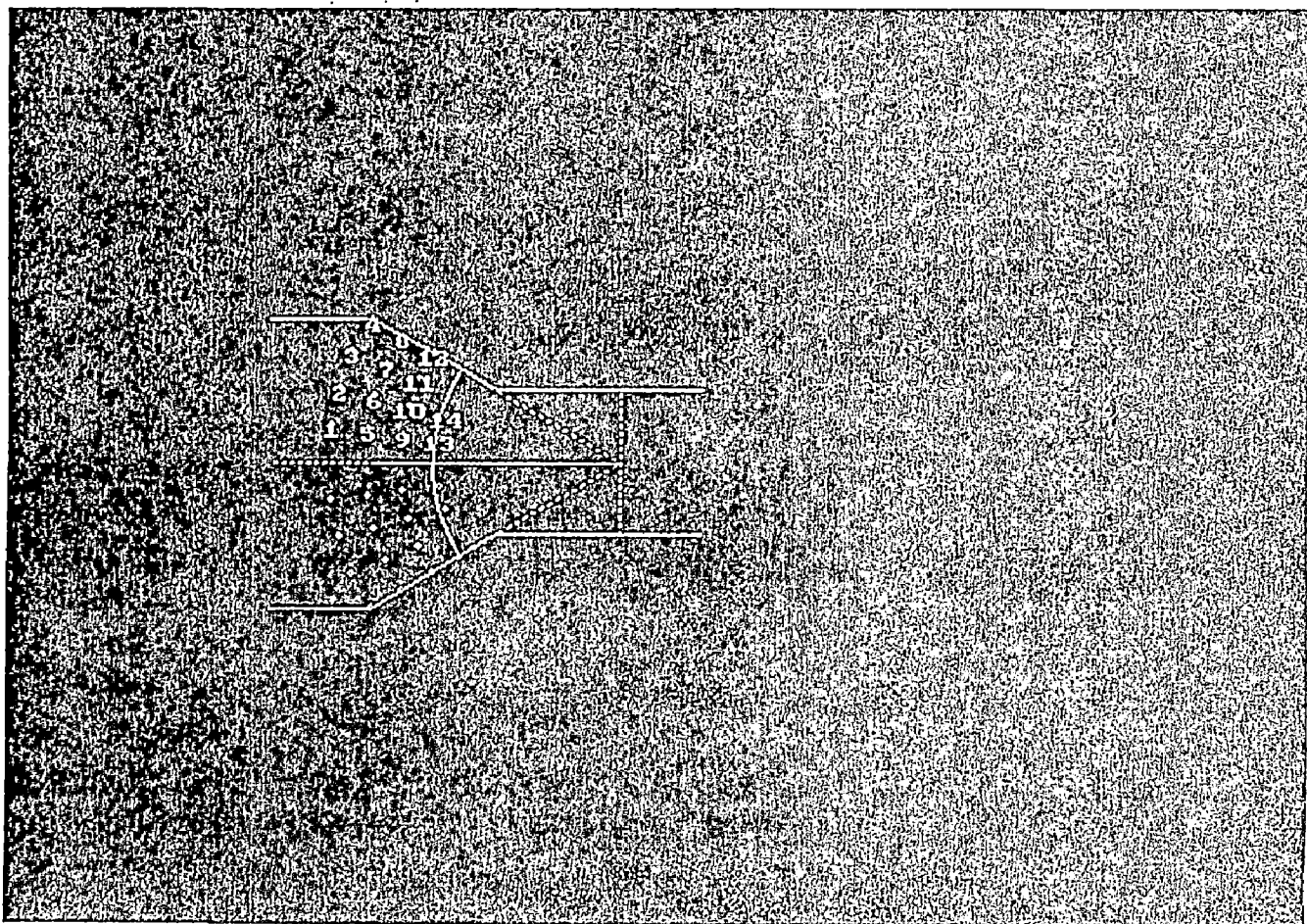


Fig.19

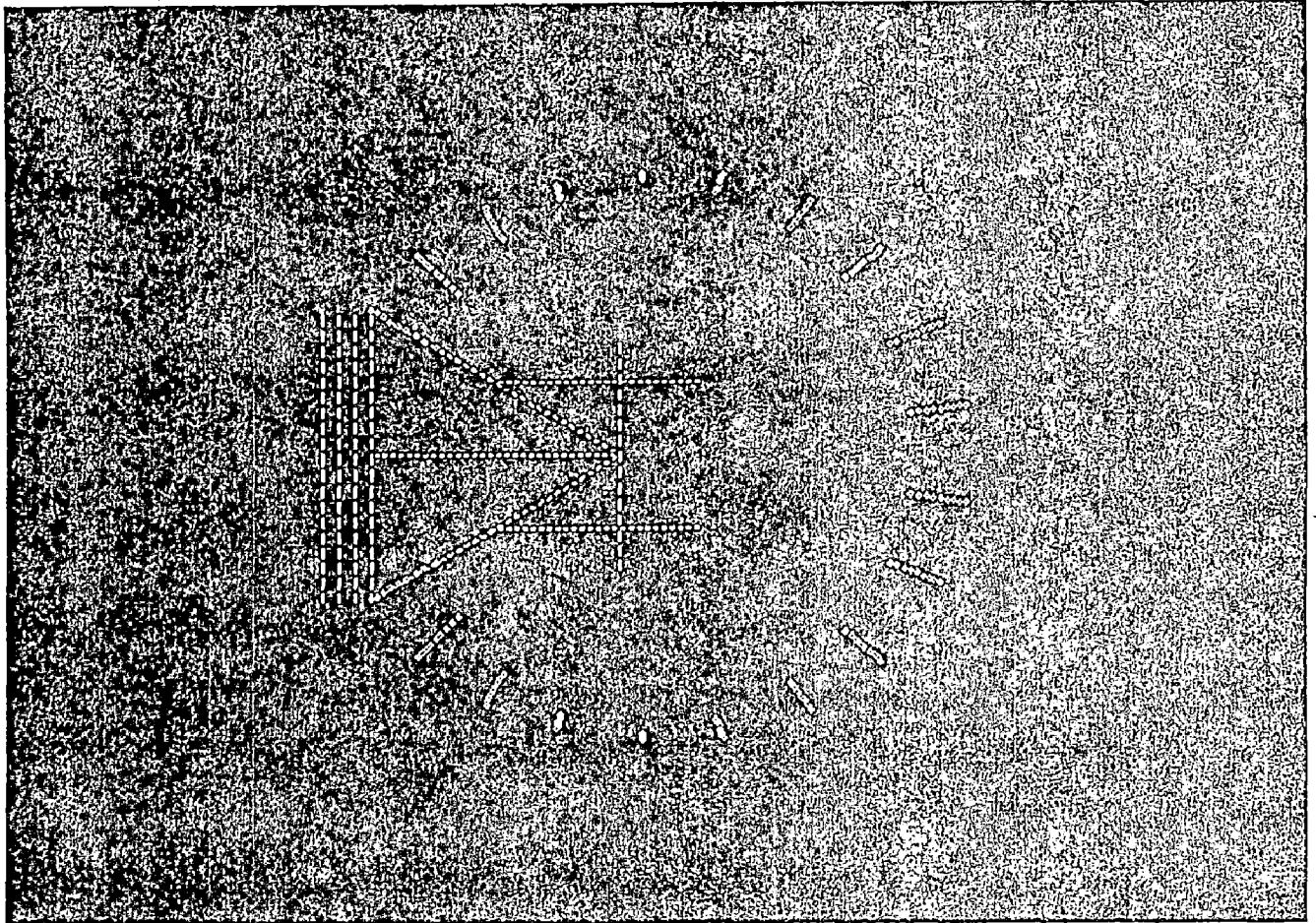


Fig.20

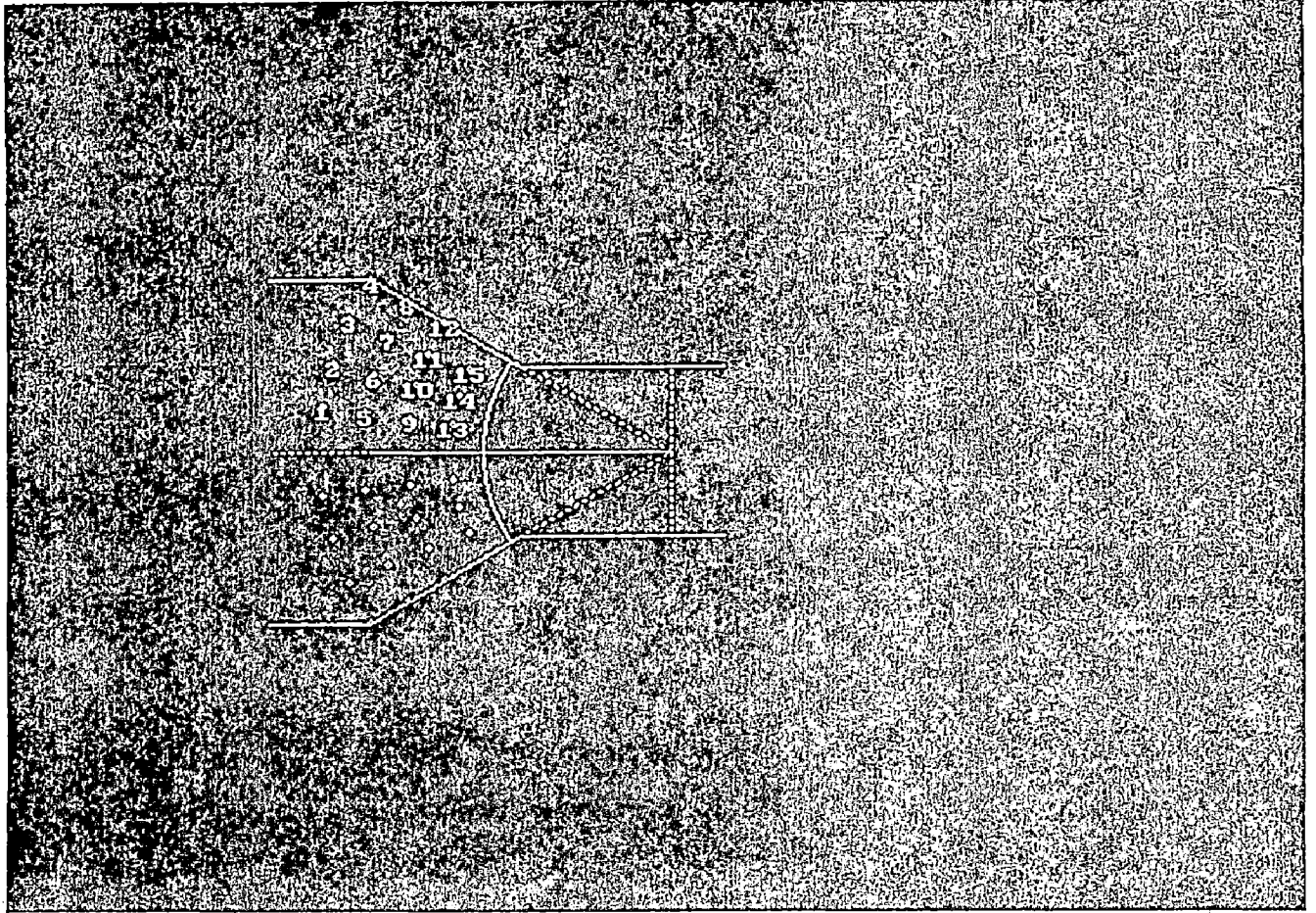


Fig.21

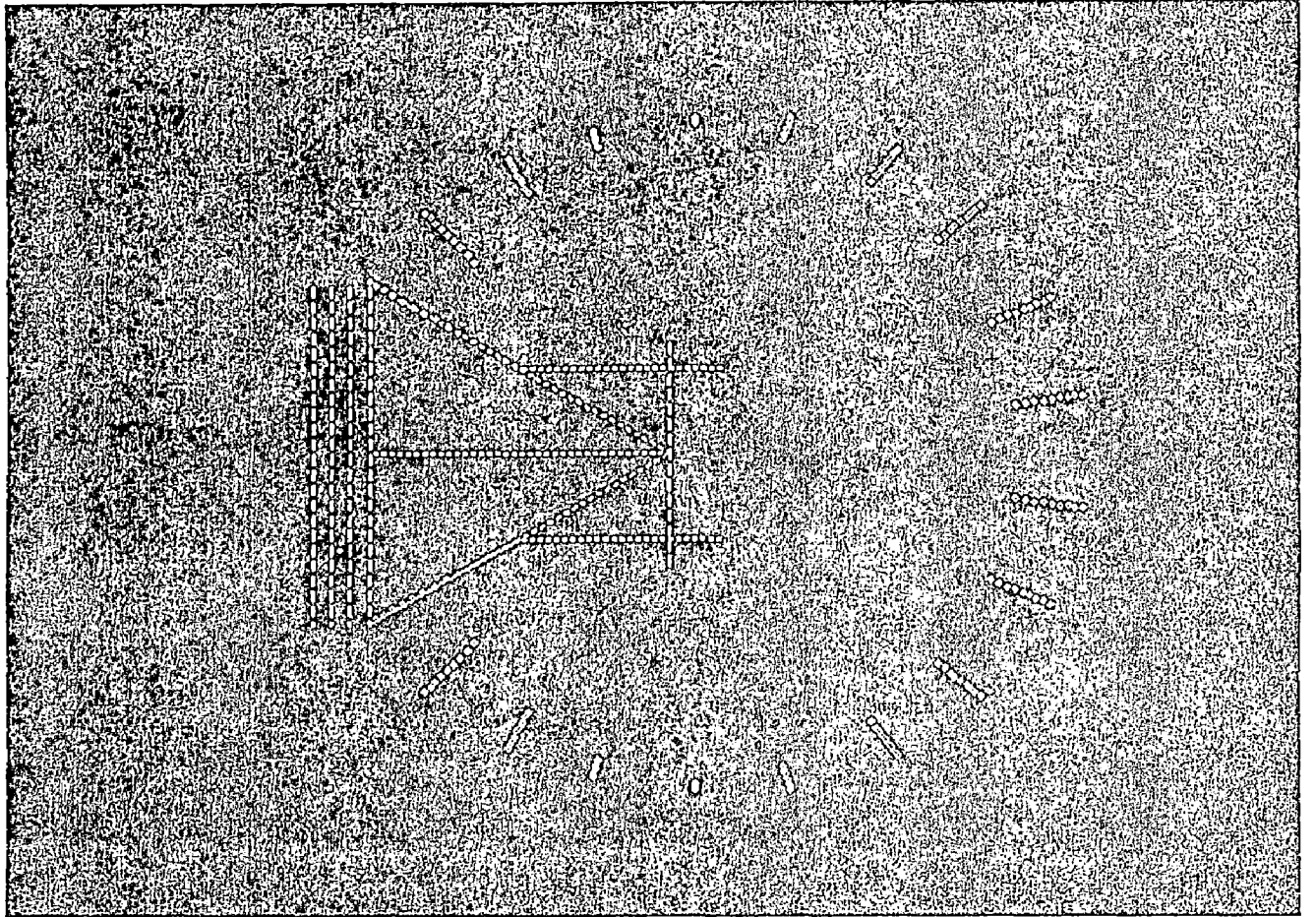


Fig.22

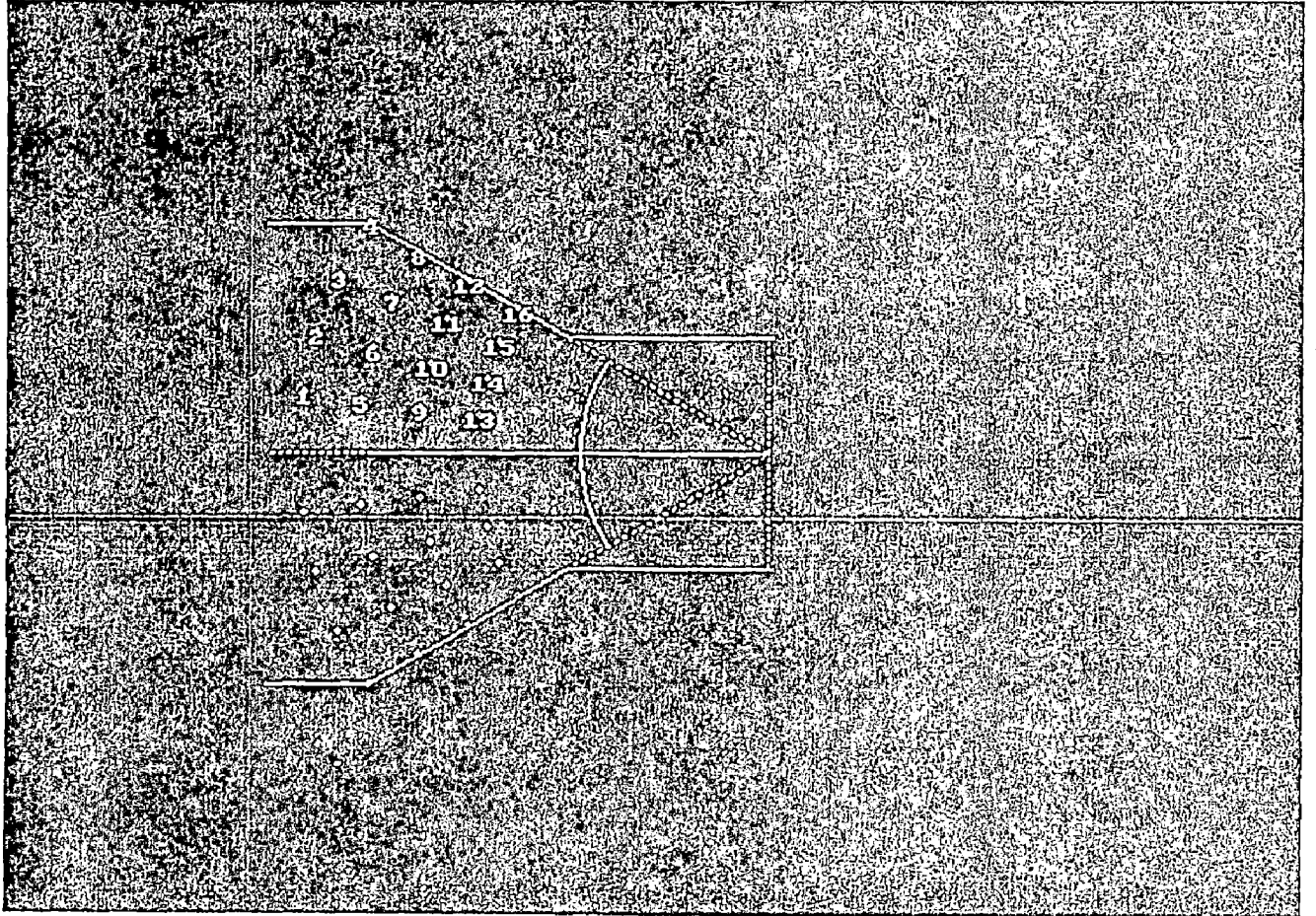


Fig.23

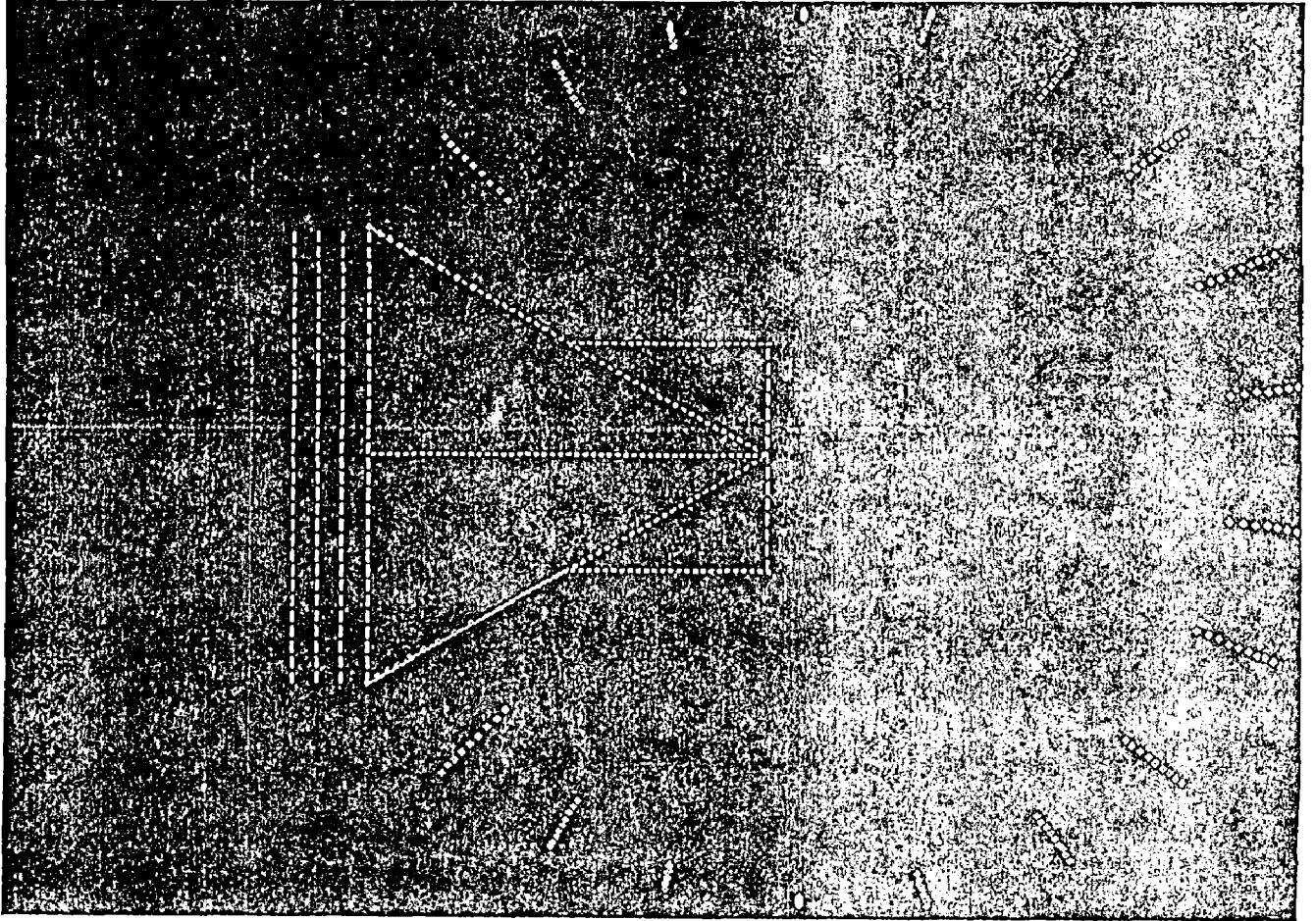


Fig.24

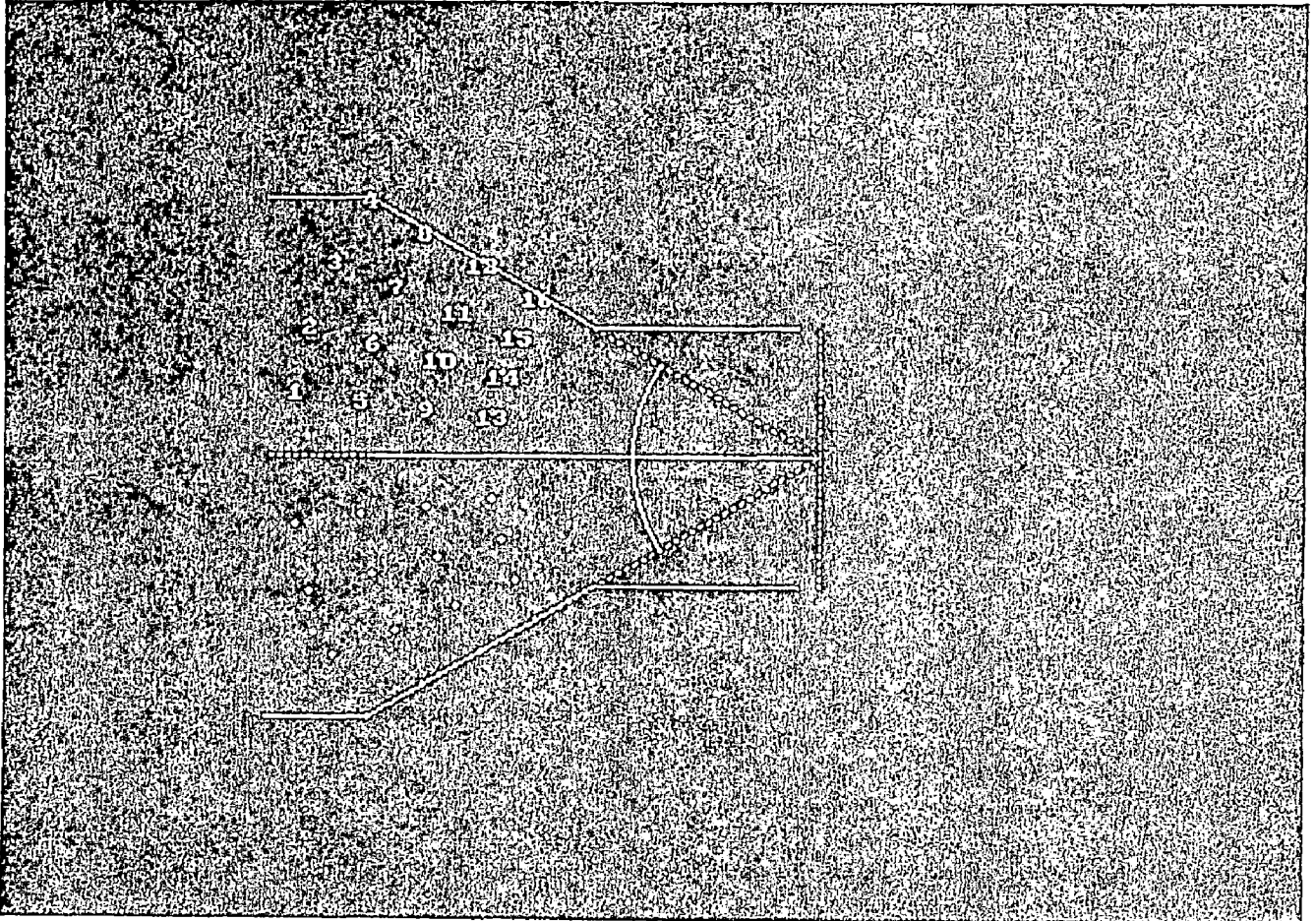


Fig.25

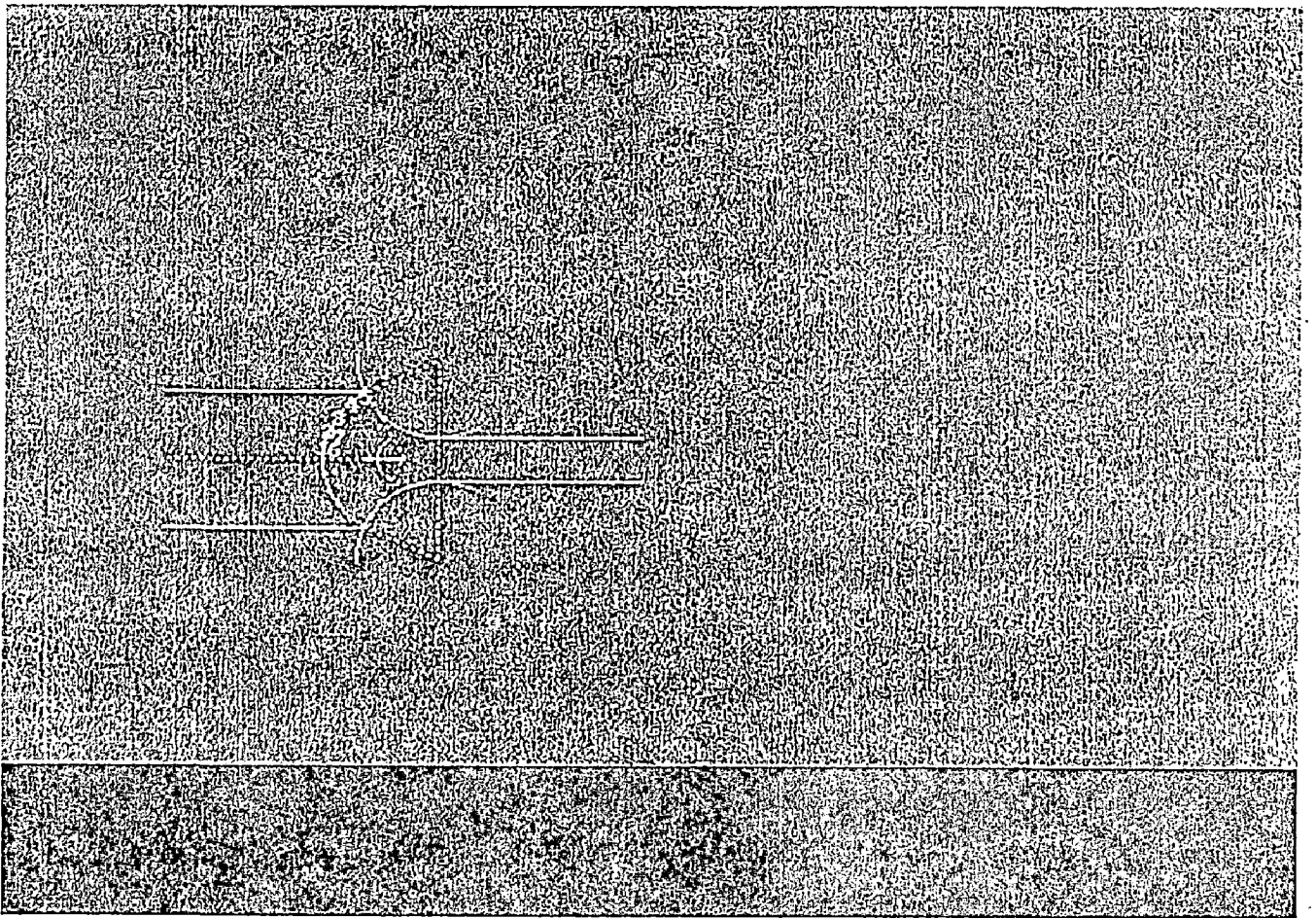


Fig.26

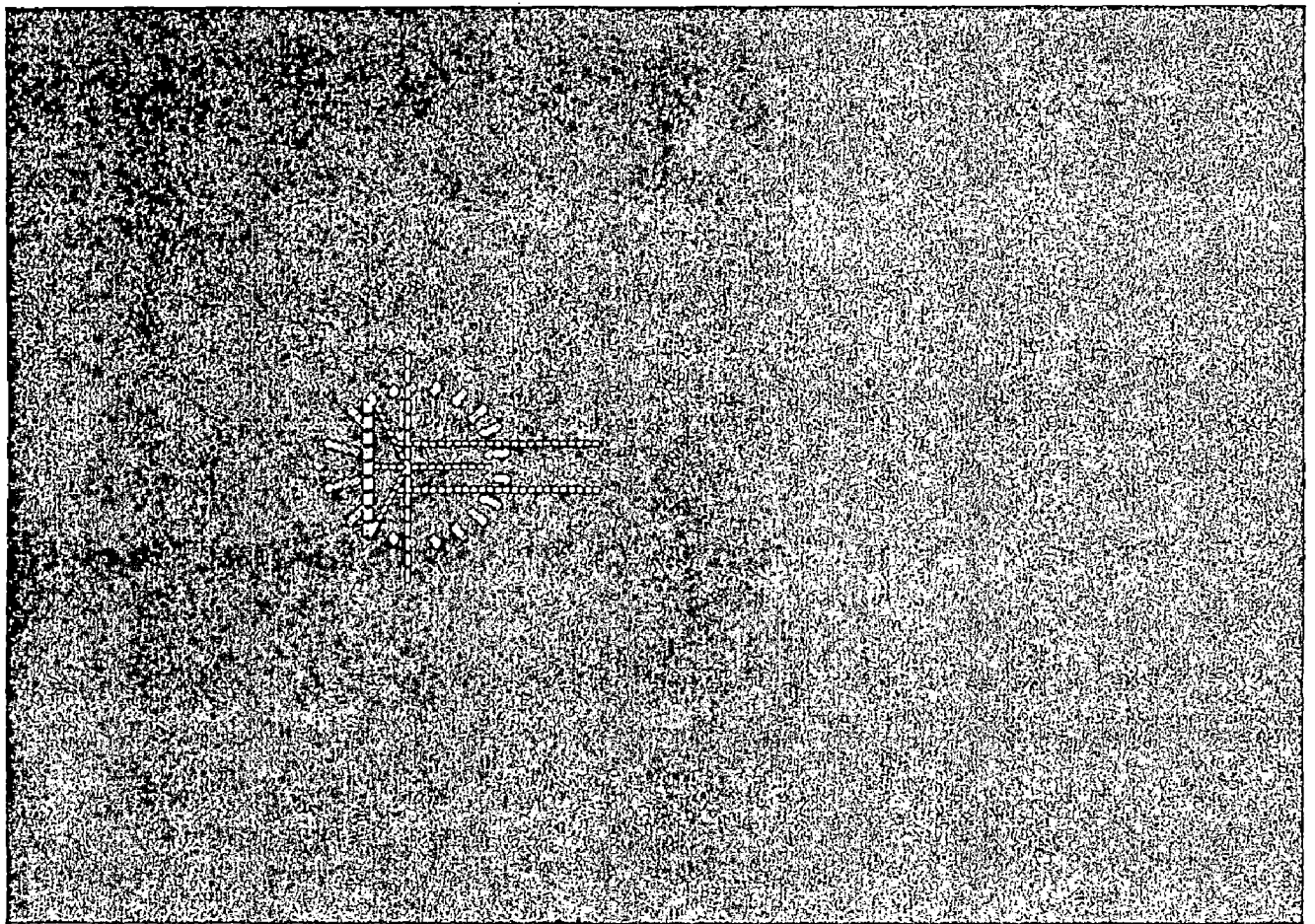


Fig.27

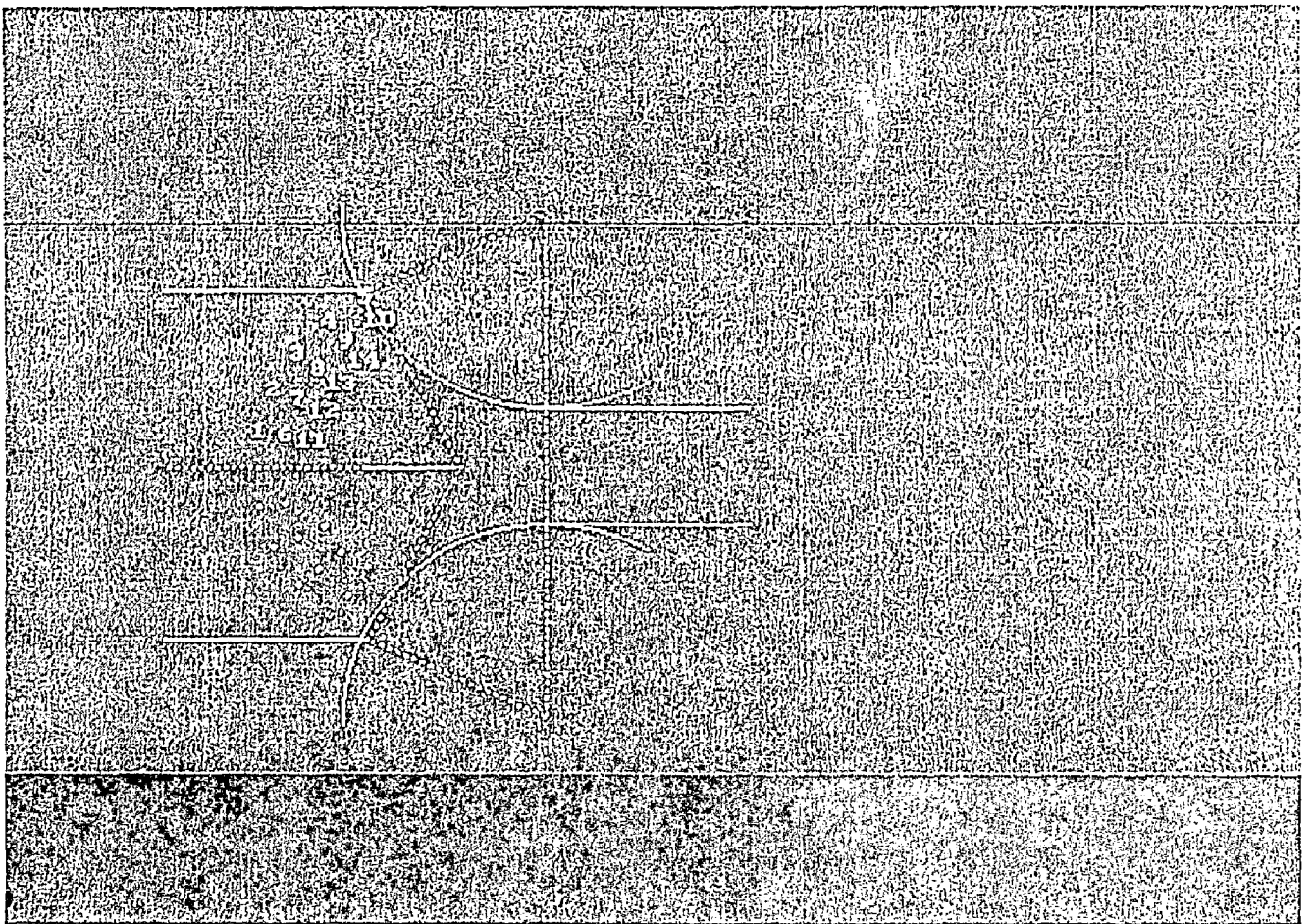


Fig.28

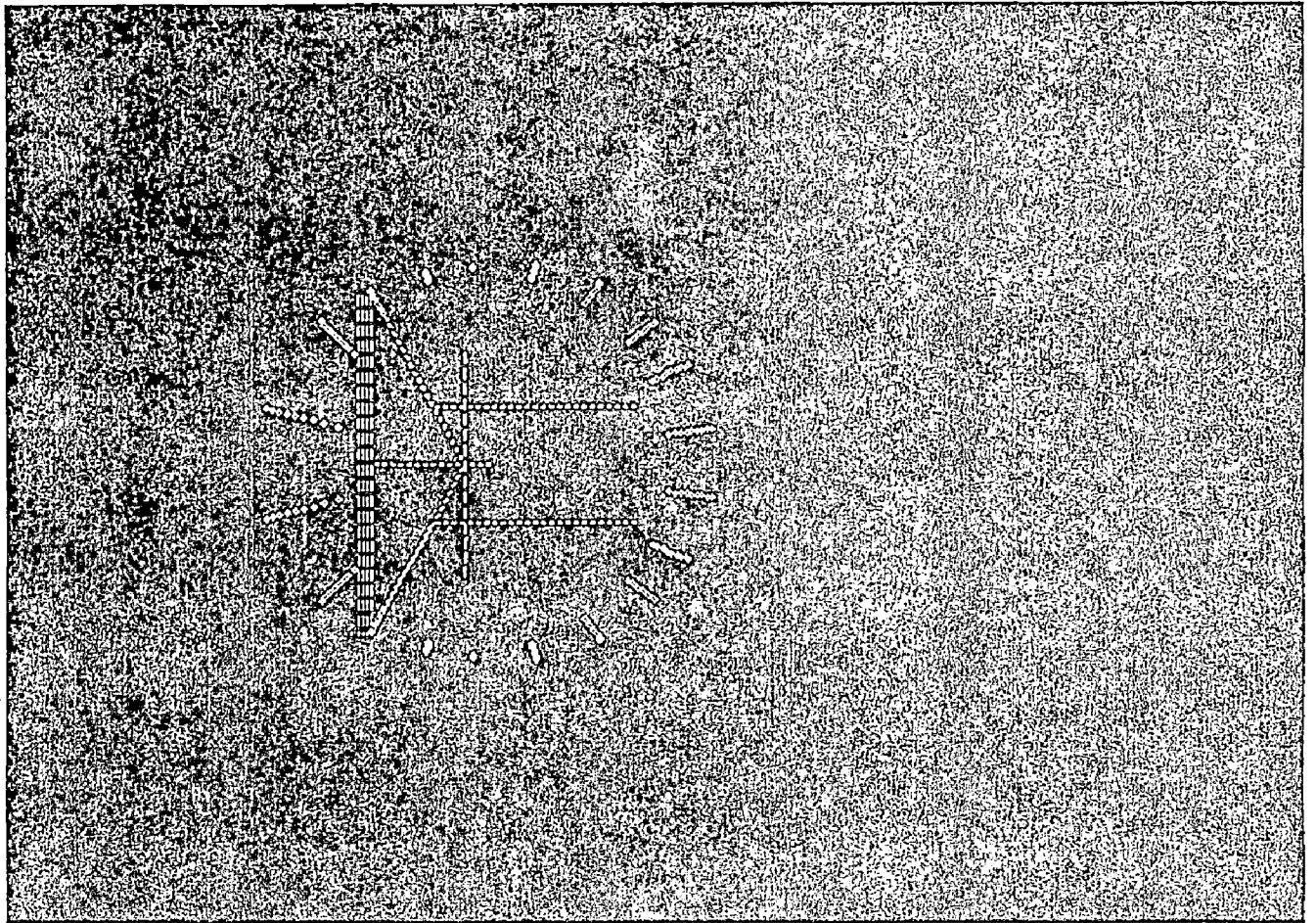


Fig.29

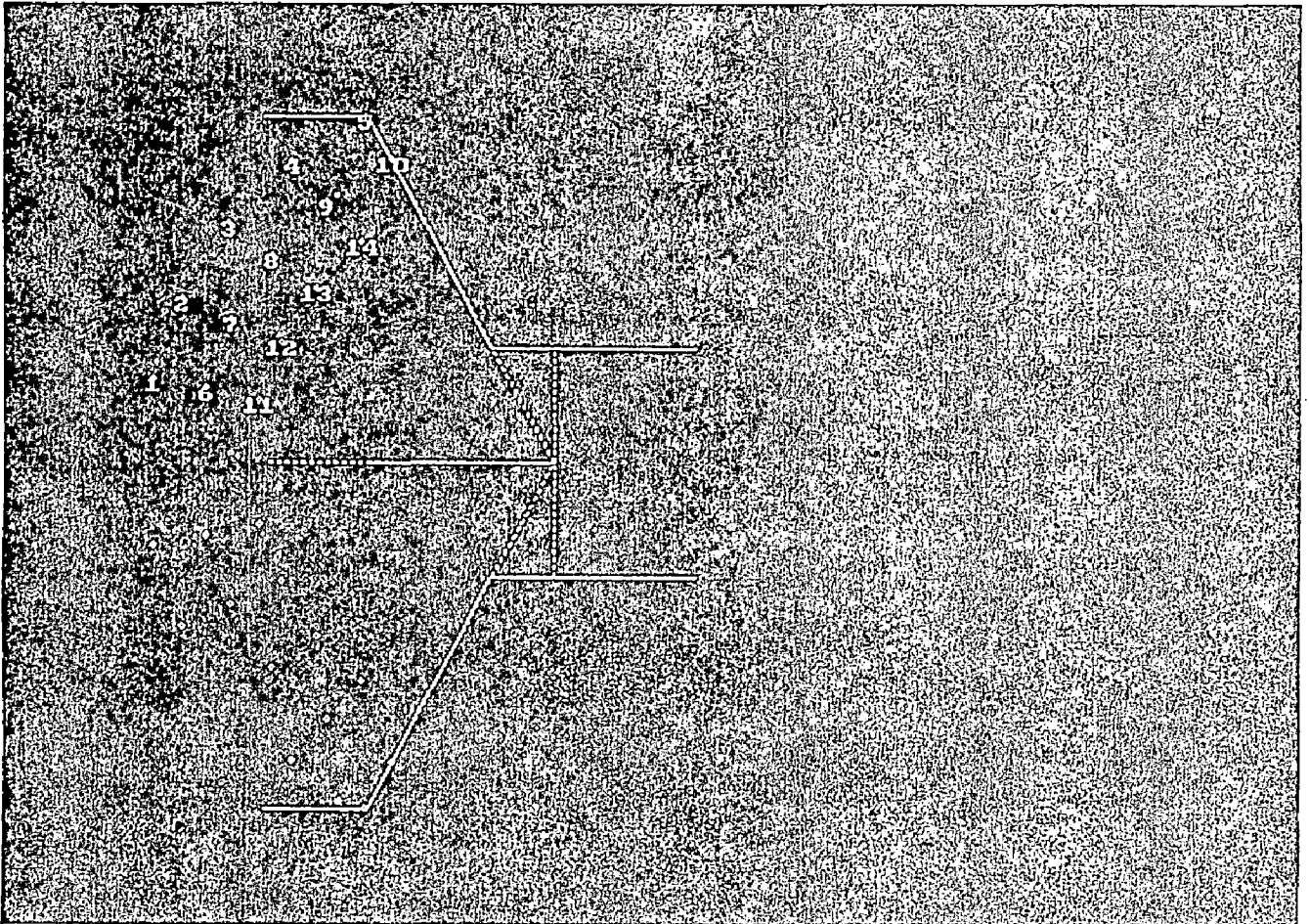


Fig.30

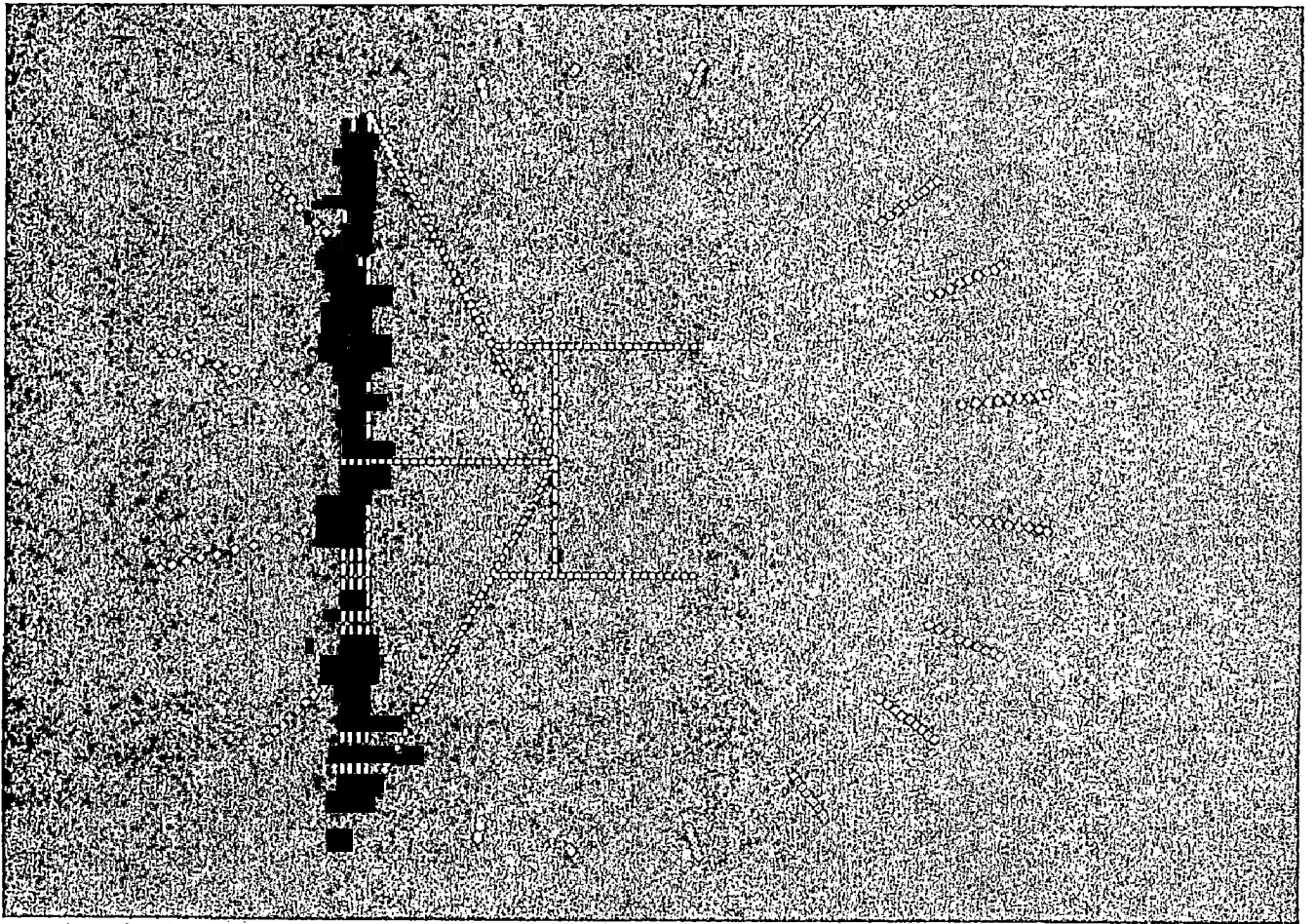


Fig.31

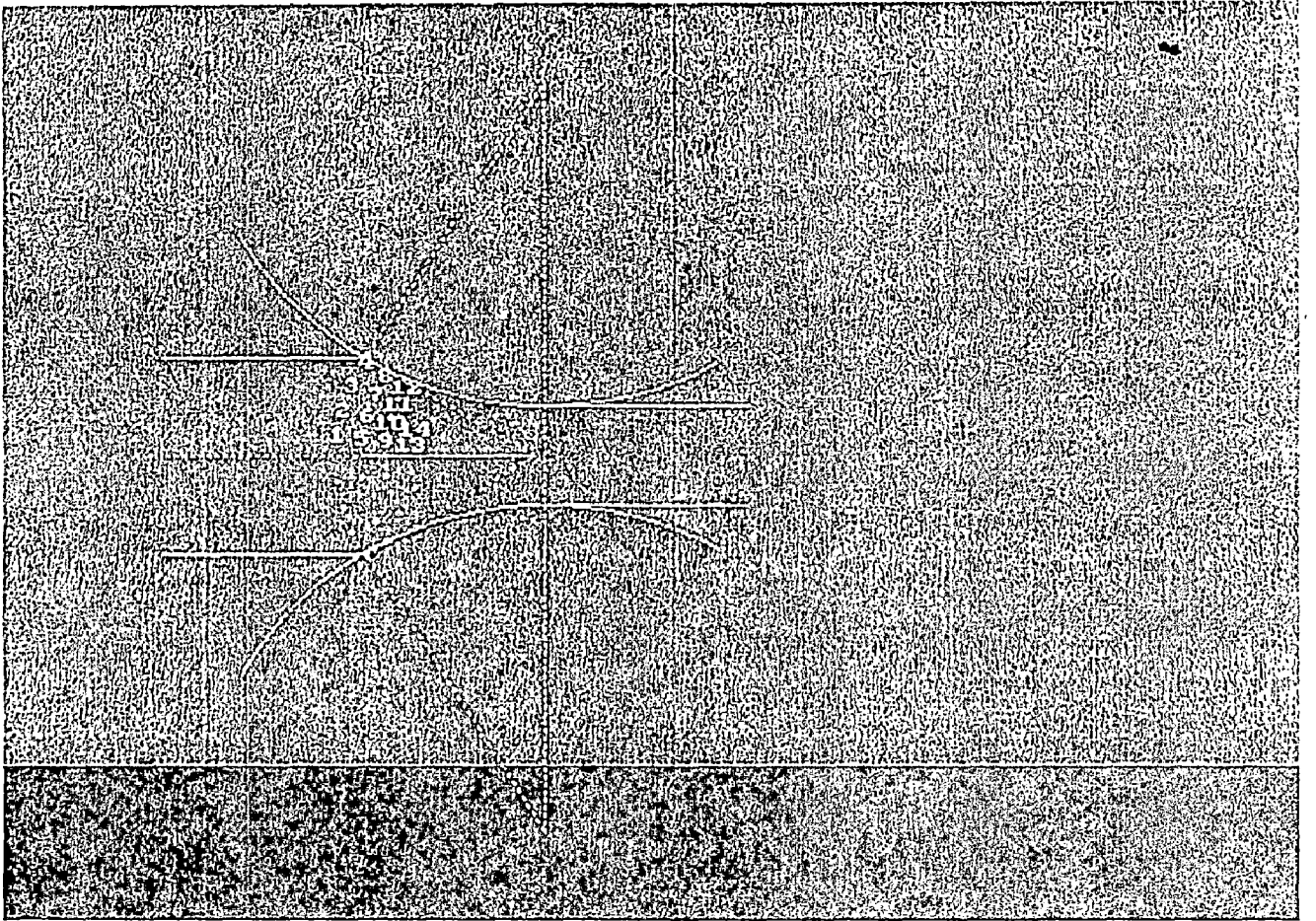


Fig. 32

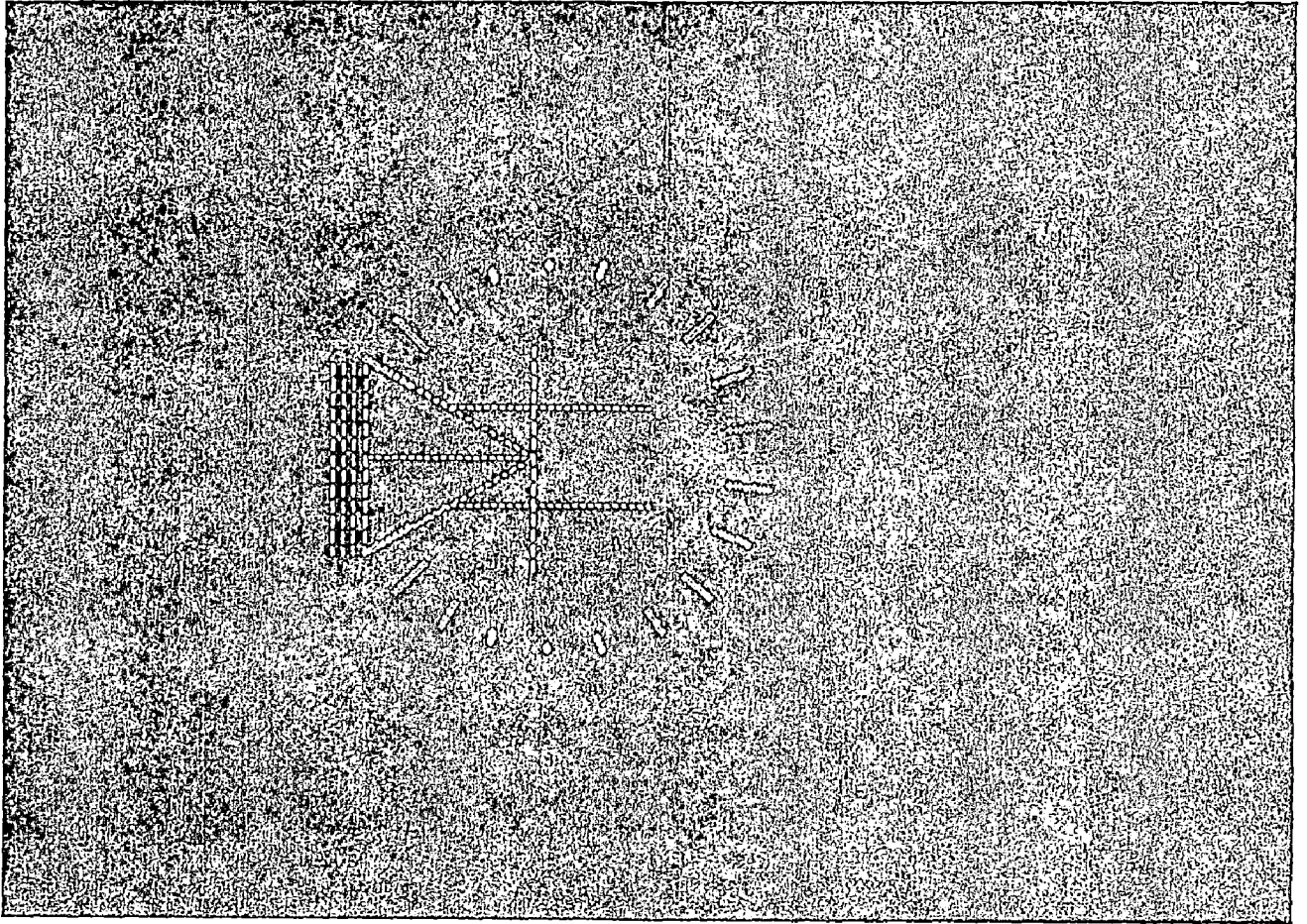


Fig. 33



Fig 34

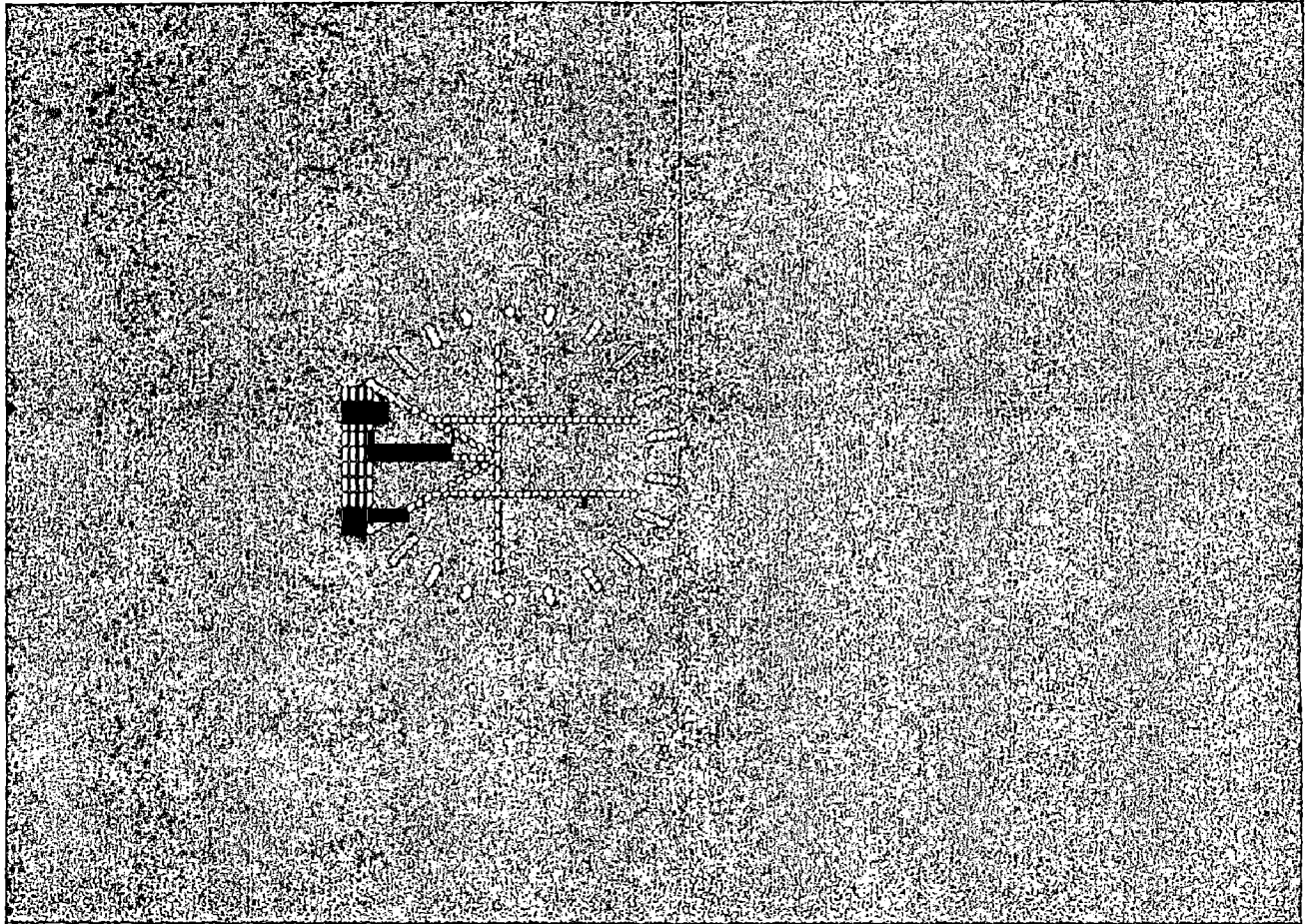


Fig. 235

TABLE - 1

S.No.	angle	radius	velocity	cr	ct
1	7.842391	5.760985	-3.855422	0.018	-0.018
2	25.095652	10.122231	-6.345178	2.304	-2.304
3	37.643478	10.122231	-4.355401	5.184	-5.184
4	50.191303	10.122231	-3.026634	9.216	-9.216
5	62.739129	10.122231	-2.173913	14.4	-14.4
6	12.547826	8.7726	-8.741259	0.576	-0.576
7	25.095652	8.7726	-6.345178	2.304	-2.304
8	37.643478	8.7726	-4.355401	5.184	-5.184
9	50.191303	8.7726	-3.026634	9.216	-9.216
10	62.739129	8.7726	-2.173913	14.4	-14.4
11	12.547826	7.422969	-8.741259	0.576	-0.576
12	25.095652	7.422969	-6.345178	2.304	-2.304
13	37.643478	7.422969	-4.355401	5.184	-5.184
14	50.191303	7.422969	-3.026634	9.216	-9.216
15	62.739129	7.422969	-2.173913	14.4	-14.4
16	12.547826	6.073339	-8.741259	0.576	-0.576
17	25.095652	6.073339	-6.345178	2.304	-2.304
18	37.643478	6.073339	-4.355401	5.184	-5.184
19	50.191303	6.073339	-3.026634	9.216	-9.216
20	62.739129	6.073339	-2.173913	14.4	-14.4
21	12.547826	4.723708	-8.741259	0.576	-0.576
22	25.095652	4.723708	-6.345178	2.304	-2.304
23	37.643478	4.723708	-4.355401	5.184	-5.184
24	50.191303	4.723708	-3.026634	9.216	-9.216
25	62.739129	4.723708	-2.173913	14.4	-14.4

TABLE - 2

Initial thickness	6
Final thickness	3
Shear factor	0.4
Grinding factor	4x4
Optimal roll radius	7.5
Magnification	1.604945e-59
Reduction Ratio	2
Final Velocity	10
Initial Velocity	5

S.No.	Angle	Radius	Velocity	er	et
1	9.055613	5.075051	-9.52381	0.266667	-0.266667
2	18.111227	5.075051	-8.333333	1.066667	-1.066667
3	27.16684	5.075051	-6.896552	2.4	-2.4
4	36.222453	5.075051	-5.555556	4.266667	-4.266667
5	9.055613	4.440669	-9.52381	0.266667	-0.266667
6	18.111227	4.440669	-8.333333	1.066667	-1.066667
7	27.16684	4.440669	-6.896552	2.4	-2.4
8	36.222453	4.440669	-5.555556	4.266667	-4.266667
9	9.055613	3.806288	-9.52381	0.266667	-0.266667
10	18.111227	3.806288	-8.333333	1.066667	-1.066667
11	27.16684	3.806288	-6.896552	2.4	-2.4
12	36.222453	3.806288	-5.555556	4.266667	-4.266667
13	9.055613	3.171907	-9.52381	0.266667	-0.266667
14	18.111227	3.171907	-8.333333	1.066667	-1.066667
15	27.16684	3.171907	-6.896552	2.4	-2.4
16	36.222453	3.171907	-5.555556	4.266667	-4.266667

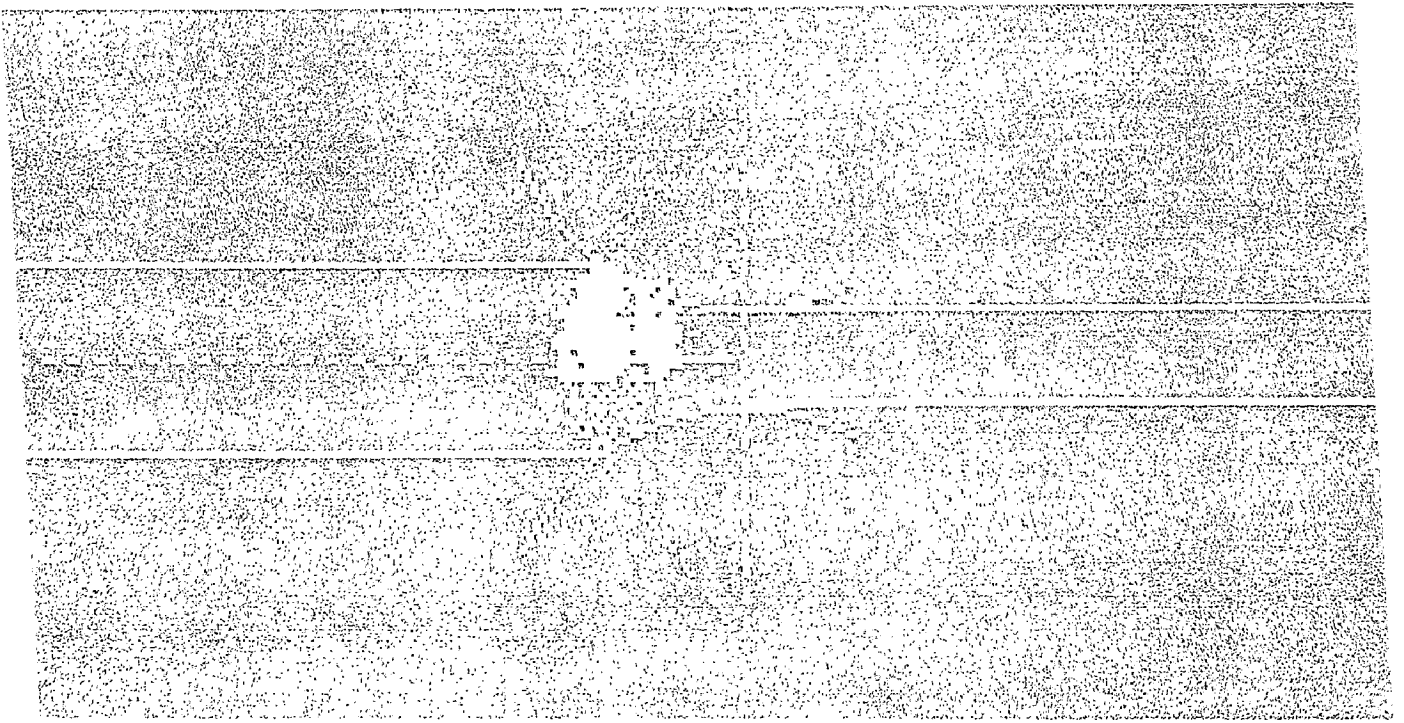


Fig. 36

TABLE - 3

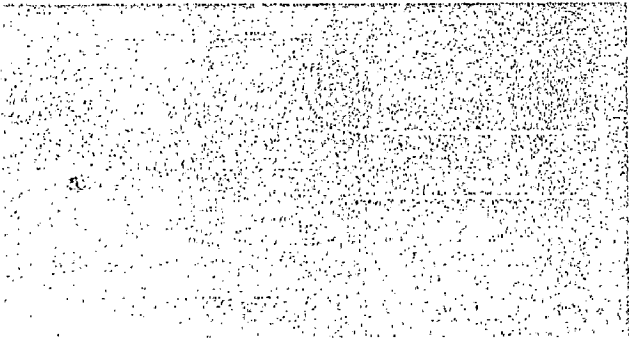


Fig. 37

initial thickness 20
 final thickness 5
 wear factor 0.4
 grinding factor 4x4
 optimal roll radius 4.166667
 magnification 1.322032e-311
 reductionRatio 4
 initial Velocity 10
 final Velocity 2.5

No.	Angle	Radius	Velocity	er	et
	27.16684	10.55801	-5.263158	12.96	-12.96
2	54.33368	10.55801	-2.173913	51.84	-51.84
3	81.50052	10.55801	-1.098901	116.64	-116.64
4	108.66736	10.55801	-0.649351	207.36	-207.36
5	27.16684	8.578383	-5.263158	12.96	-12.96
6	54.33368	8.578383	-2.173913	51.84	-51.84
7	81.50052	8.578383	-1.098901	116.64	-116.64
8	108.66736	8.578383	-0.649351	207.36	-207.36
9	27.16684	6.598756	-5.263158	12.96	-12.96
10	54.33368	6.598756	-2.173913	51.84	-51.84
11	81.50052	6.598756	-1.098901	116.64	-116.64
12	108.66736	6.598756	-0.649351	207.36	-207.36
13	27.16684	4.61913	-5.263158	12.96	-12.96
14	54.33368	4.61913	-2.173913	51.84	-51.84
15	81.50052	4.61913	-1.098901	116.64	-116.64
16	108.66736	4.61913	-0.649351	207.36	-207.36

TABLE - 4

thickness 24
 thickness 4
 r factor 0.4
 ng factor 4x4
 nal roll radius 2
 ification` -5.212002e+304
 ction Ratio 6
 Velocity 10
 l Velocity 1.666667

α.	angle	radius	veocity	er	et
	45.278066	-580.171717	-2.105263	125	-125
	90.556133	-580.171717	-0.625	500	-500
	135.834199	-580.171717	-0.28777	1125	-1125
	181.112266	-580.171717	-0.163934	2000	-2000
	45.278066	-459.302609	-2.105263	125	-125
	90.556133	-459.302609	-0.625	500	-500
	135.834199	-459.302609	-0.28777	1125	-1125
	181.112266	-459.302609	-0.163934	2000	-2000
	45.278066	-338.433502	-2.105263	125	-125
	90.556133	-338.433502	-0.625	500	-500
	135.834199	-338.433502	-0.28777	1125	-1125
	181.112266	-338.433502	-0.163934	2000	-2000
	45.278066	-217.564394	-2.105263	125	-125
	90.556133	-217.564394	-0.625	500	-500
	135.834199	-217.564394	-0.28777	1125	-1125
	181.112266	-217.564394	-0.163934	2000	-2000



Fig. 38